Natural Science Report, Ochanomizu University, Vol. 11, No. 2, 1960
お茶の水女子大学 自然科学報告 第11巻 第2号

On the Relations between the Diffusion Parameters and Meteorological Conditions

Jiro Sakagami (坂上治郎)

Department of Physics, Faculty of Science,
Ochanomizu University, Tokyo

Introduction

Explicit formulae for concentrations of diffusive matters emitted in the atmosphere have been published by Roberts,[1] Sutton,[2] Bosanquet-Pearson[3] and others. But there still remain some problems.

The first problem is that, whether the functional forms of the formulae can express truely the actual state of diffusion. The second problem is that, under prescribed meteorological conditions, that values should be adopted for the parameters contained in the formulae. At the same time, it becomes an important problem, what kind of quantity should be suitable in order to designate the meteorological state.

As for the first problem, Sutton's formulae published in 1932[2] have been chiefly treated. After then, many researchers have made comments about the check for the vertical concentration distribution, but almost of all have not shown quantitatively the degree of agreement with the observed results; even the figures in Hay-Pasquill's paper,[4] with which they insist that the Sutton's formula agrees fairly good, show some systematic deviations.

The author discontented with disagreements, considered different formulae in 1941[5] and they were useful for analyses of may field experiments.(1)

As for the second problem, there have been rather many reports which determined the values of Sutton's parameters,[6,7] but they did not show distinctly to what extent the formulae with the determined parameter values, could reproduce the observed results of concentration over the whole area of experiments; and moreover, the resulted values of parameters scattered considerably.

Meteorological states have been classified in some case only in lapse, neutral and inversion; or designated by the stability ratio, the stability length; or classified by synthetic classification based on insolation, wind speed etc. It has not been verified quantitatively that these classifications are adequate.

(1) All reports and data have been lost at the End of the II War.

Many theoretical works have been carried out, but they relied upon the other author's synthetical results whose errors did not show distinctly.

These unsatisfactory situations are entirely due to insufficiency of experimental results. There have been only few field experiments of diffusion, because they are too expensive and too laborious. Recently some detailed experimental data, including those of the Tokai-experiments carried out by the Investigation Committee for Atomic Energy and Meteorology in Japan, have been published. Among them, data of Project Prairie Grass, carried out in the United States, contain many runs of experiments, many observation-posts and detailed micrometeorological observations. Treating with these data, we could check the formulae and analyse the relation between the diffusion parameters in the formulae and the meteorological parameters.

The chief object of this paper is to compare the theoretical results with the pure experimental data and to show their adequateness objectively by graphs.

Diffusion formulae

A) *Sutton's formula.* According to the well known Sutton's formula for a continuous point source whose height is h above the ground, concentration χ at a position, x, y, z, is expressed by

$$\chi=\frac{Q}{u}\frac{e^{-\frac{y^2}{A}}}{\sqrt{A\pi}}\left(e^{-\frac{(h+z)^2}{B}}+e^{-\frac{(h-z)^2}{B}}\right)$$

$$A=c_y^{\,2}x^{2-n},\quad B=c_z^{\,2}x^{2-n} \qquad (1),$$

where Q is the source intensity; x: leeward distance from the source; y: cross wind distance from the mean wind direction; z: vertical height from the ground; u: mean wind speed; and c_y, c_z and are Sutton's diffusion parameters.

B) *The author's formula.* The author adopted the following differential equation:

$$\frac{\partial\chi}{\partial t}=a_0(t)\left(\frac{\partial^2\chi}{\partial x^2}+\frac{\partial^2\chi}{\partial y^2}\right)+\frac{\partial}{\partial z}\left(b_0(t)\frac{\partial\chi}{\partial z}\right) \qquad (2)$$

and the solution which corresponds to eq. (1) is

$$\chi=\frac{Q}{u}e^{-\frac{y^2}{A}}e^{-\frac{h+z}{B}}J_0\left(i\frac{2\sqrt{hz}}{B}\right)$$

$$A=a(x),\quad B=b(x),\quad x=ut \qquad (3),$$

where J_0 is the zero order Bessel function of the 1st kind and i is

the imaginary unit.[2]

C) *Comparison with observed data.* Both equations above mentioned differ in the main the functional forms concerning vertical concentration distributions. The experimental data of vertical concentration profiles at Harwell have been reported by Stewart et al.[6] Inserting suitable values into B in equations (1) and (2), we could calculated the theoretical profiles for each leeward distances. The observed values and the calculated curves are shown in Fig. 1. The curves calculated

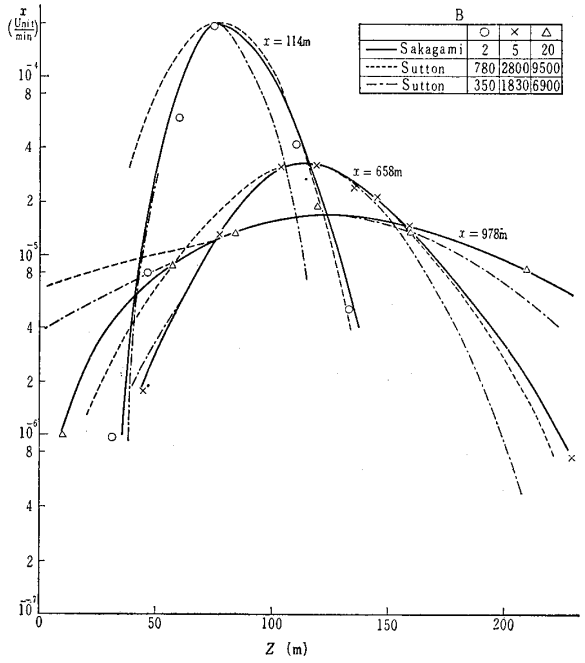

Fig. 1. Comparison of Sutton's formula with the author's one.

from eq. (1), whose lower parts fit to the observed points, do not fit to upper parts, while the curves whose upper parts fit to the observed points do not fit to lower parts; meanwhile the curves calculated from eq. (2) fit to the observed points over all range.

Other examples of comparison will be shown later.

Project Prairie Grass

58 experiments, ranging over up to 800 m from the source, were carried out at O'Neill, Nebraska in July and August 1956, and they are called Project Prairie Grass; and some reports analysing these results were published by Cramer,[8] Barad[9] and others. Pure data of the observations were published by Barad[10] at the end of last year. However, runs in which the measurements of horizontal concentration

(2) In this paper some modifications concerning the time dependency of the diffusion coefficents are made.

profiles, those of vertical concentration and the micrometeorological observations were carried in the same time, were 33; we analysed those data chiefly by the author's formulae.

Horizontal concentration profiles

As shown in Fig. 2, horizontal profiles at $x=50$ or 100 m almost always take forms of normal distributions, and the curves of log χ against y^2 show straight lines (Fig. 3); but at further distances, they gradually show some deviations from the normal distributions, and the curves in Fig. 2 become to show plateau type. We have reported[11] that, by taking a suitable moving average from quick running wind-direction records, we could explain the peculiar forms of profiles.

We shall summarize that consideration: The effects of wind directions on the horizontal concentration profiles at larger distances may be assumed to exert uniformly over the whole field of observation.

Let the wind at the source be expressed by a vector $\tilde{s}(t)$. Accord-

Fig. 2. Horizontal concentration profiles.
(○: 50 m, △: 100 m, ×: 200 m, □: 400 m, +: 800 m).

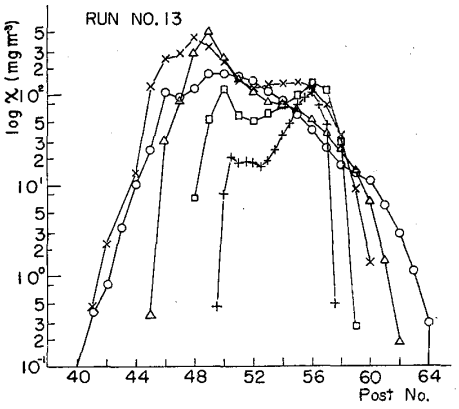

Fig. 2-1.

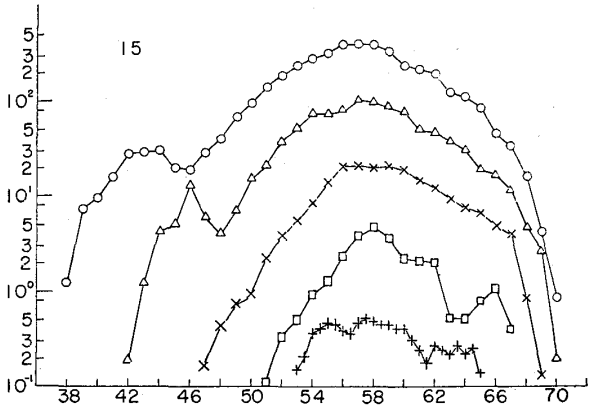

Fig. 2-2.

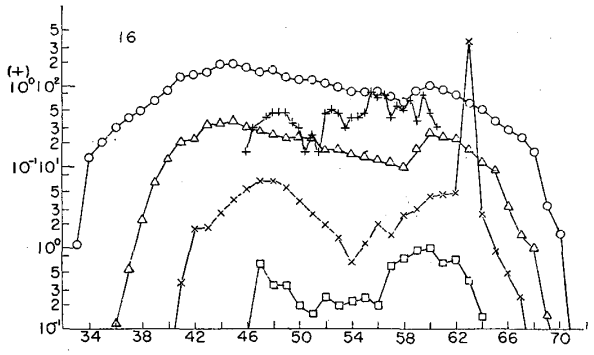

Fig. 2-3.

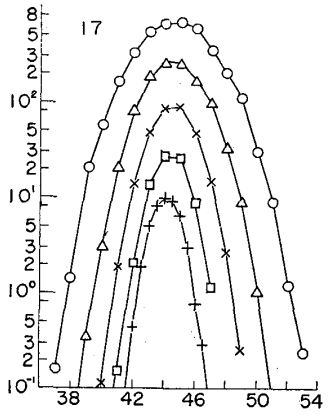

Fig. 2-4.

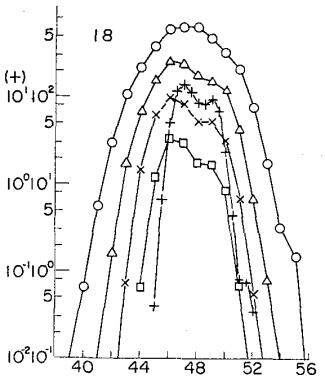

Fig. 2-5.

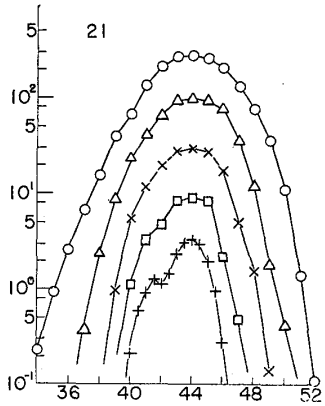

Fig. 2-6.

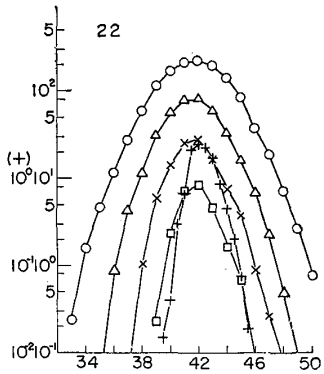

Fig. 2-7.

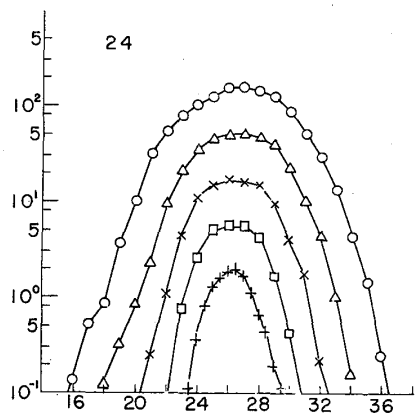

Fig. 2-8.

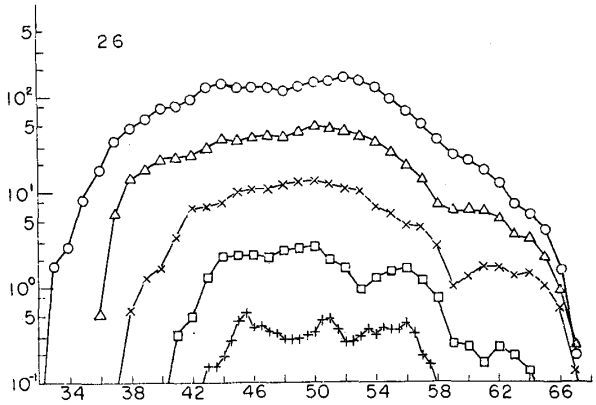

Fig. 2-9.

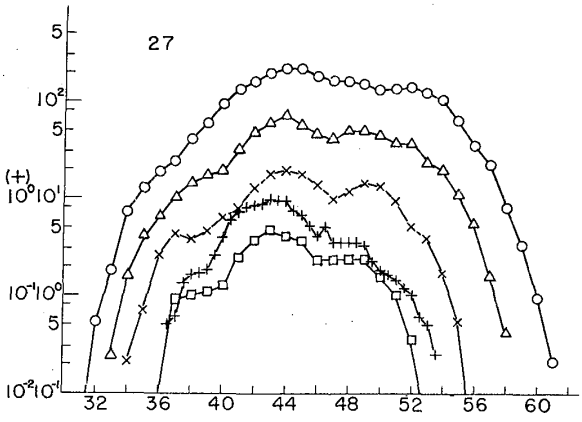

Fig. 2-10.

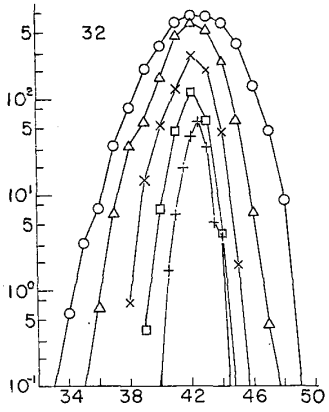

Fig. 2-11.

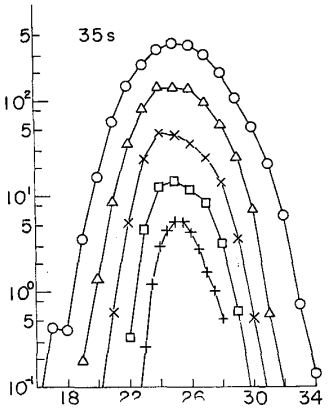

Fig. 2-12.

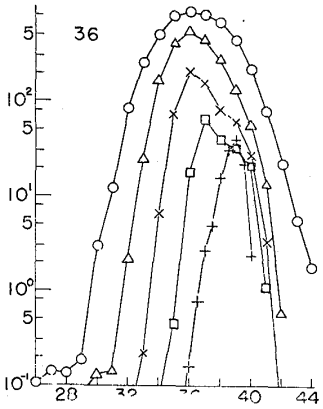

Fig. 2-13.

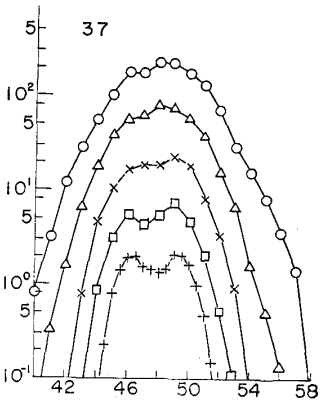

Fig. 2-14.

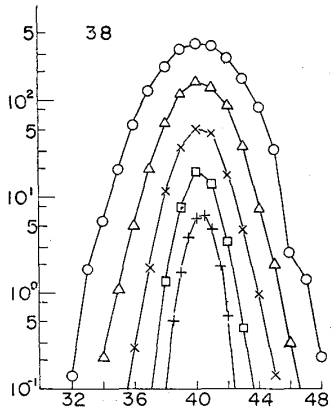

Fig. 2-15.

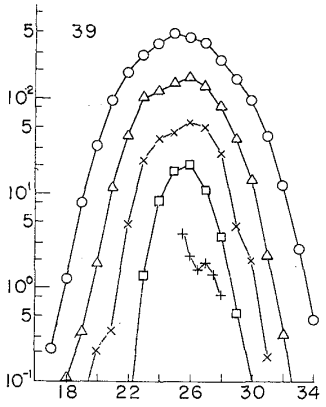

Fig. 2-16.

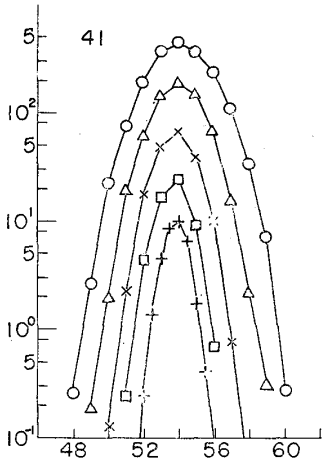

Fig. 17.

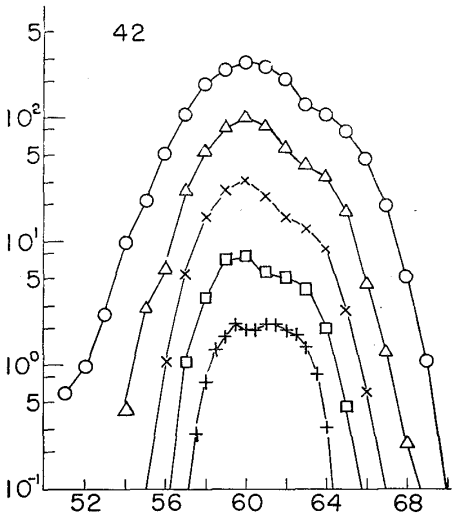

Fig. 2-18.

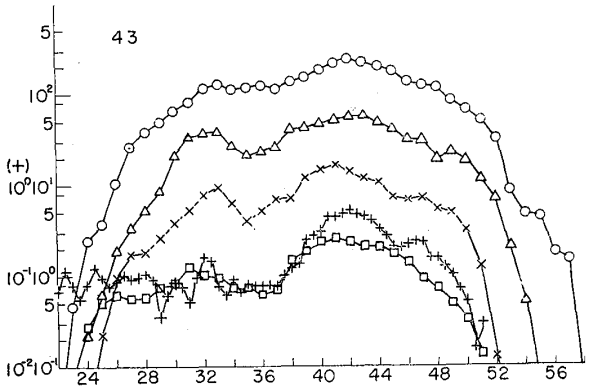

Fig. 2-19.

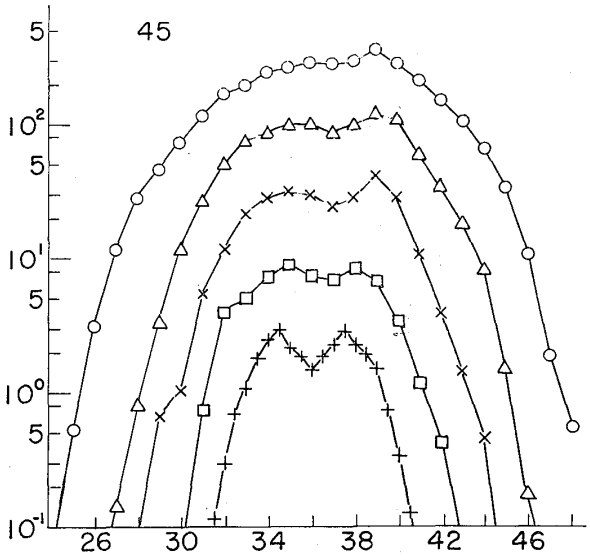

Fig. 2-20.

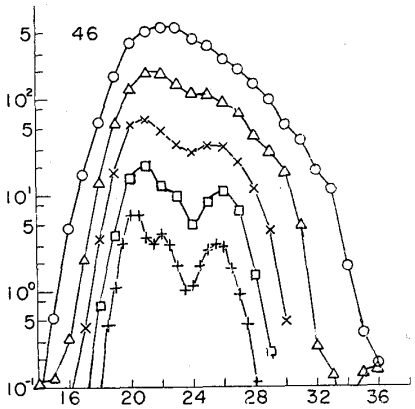

Fig. 2-21.

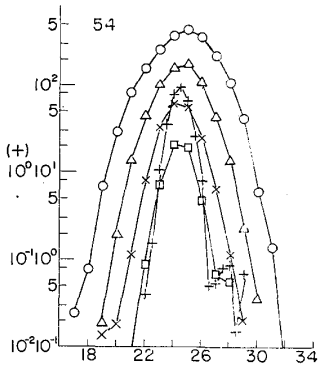

Fig. 2-22.

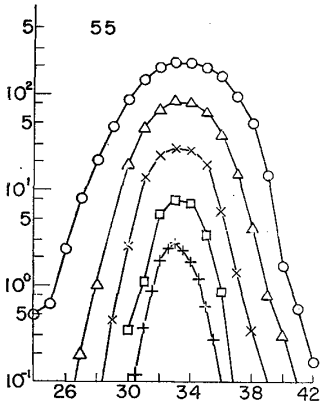

Fig. 2-23.

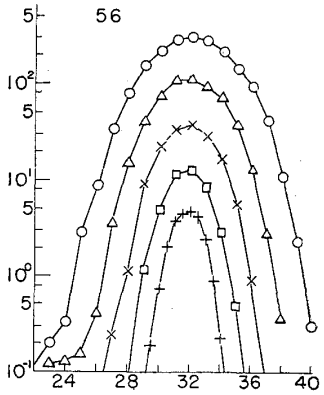

Fig. 2-24.

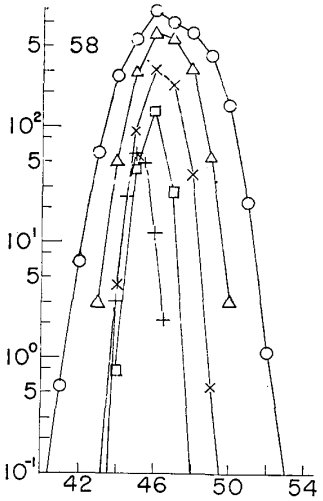

Fig. 2-25.

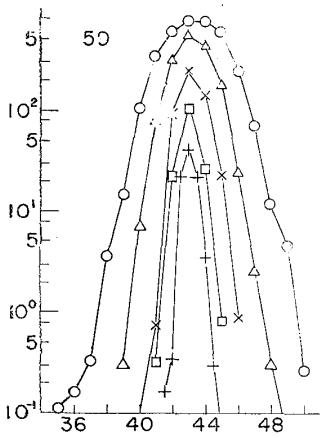

Fig. 2-26

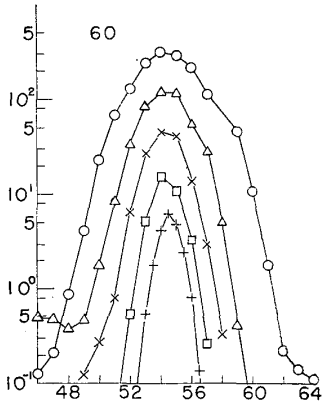

Fig. 2-27.

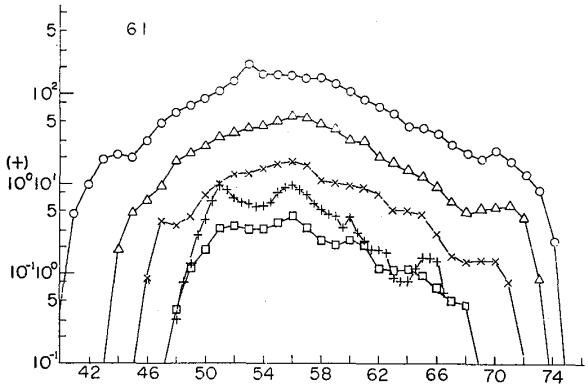

Fig. 2-28.

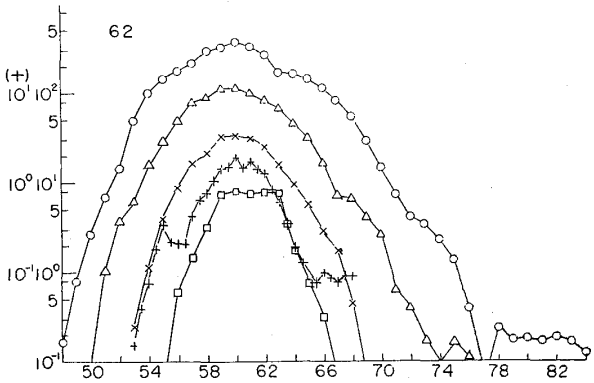

Fig. 2-29.

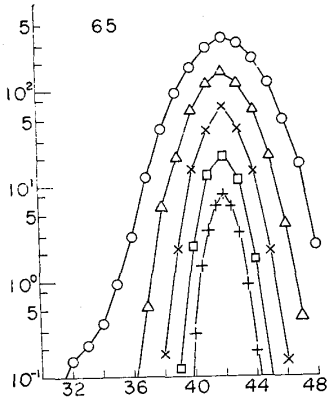

Fig. 2-30.

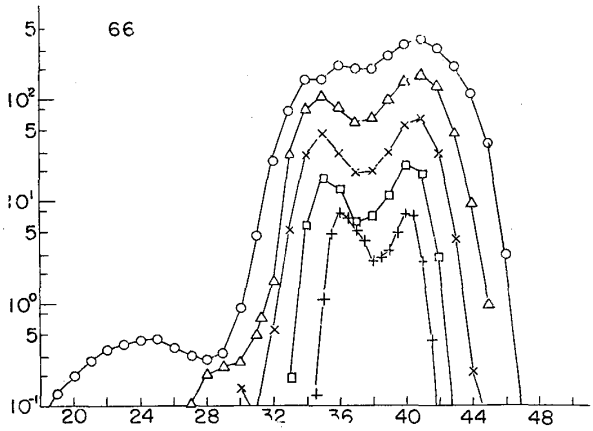

Fig. 2-31.

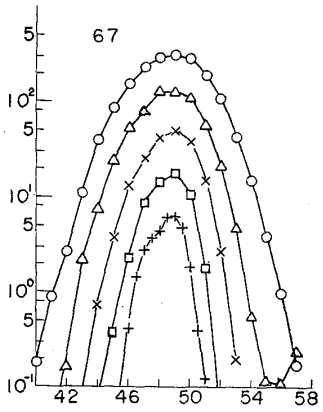

Fig. 2-32.

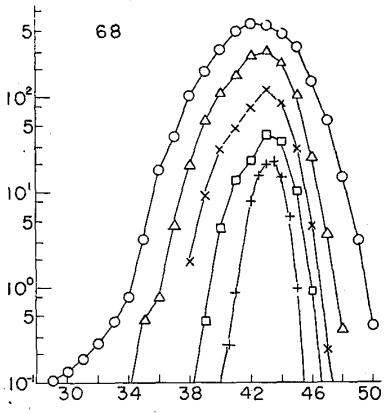

Fig. 2-33.

Fig. 3. Curves of log χ against y^2.
(○: 50 m, △: 100 m, ×: 200 m, +: 400 m, □: 800 m).

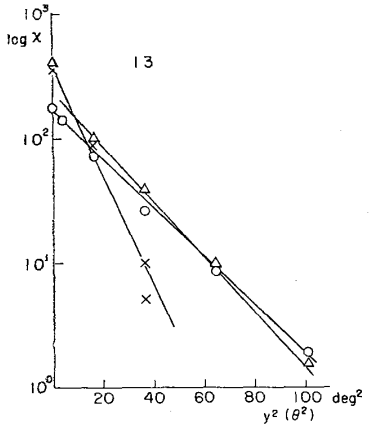

Fig. 3-1.

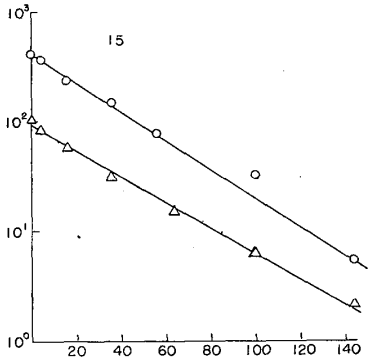

Fig. 3-2.

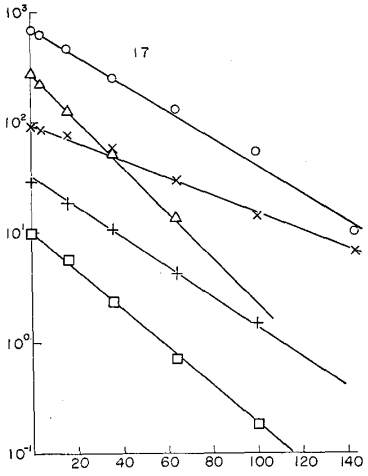

Fig. 3-3.

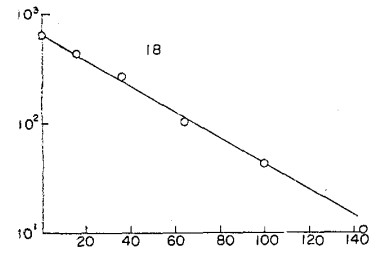

Fig. 3-4.

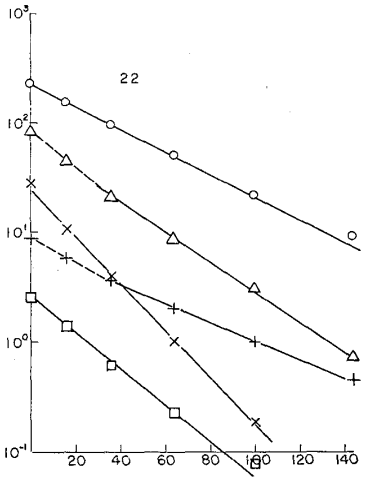

Fig. 3-5.

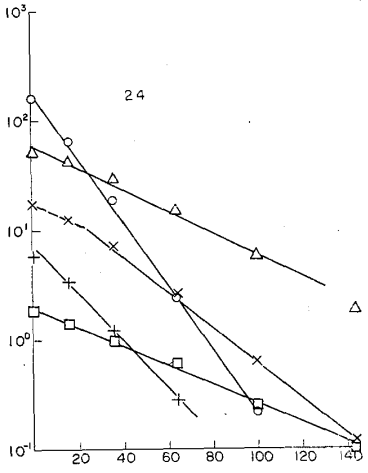

Fig. 3-6.

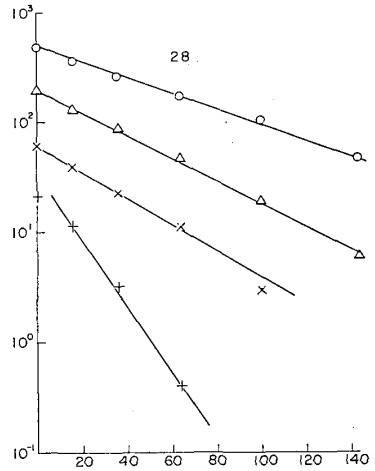

Fig. 3-7.

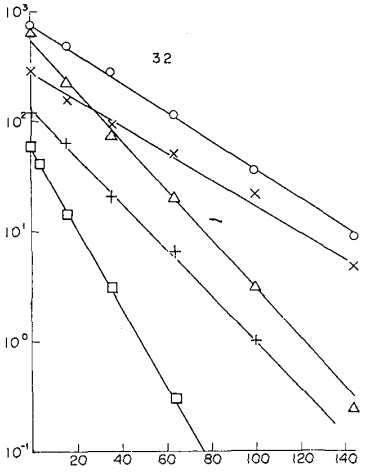

Fig. 3-8.

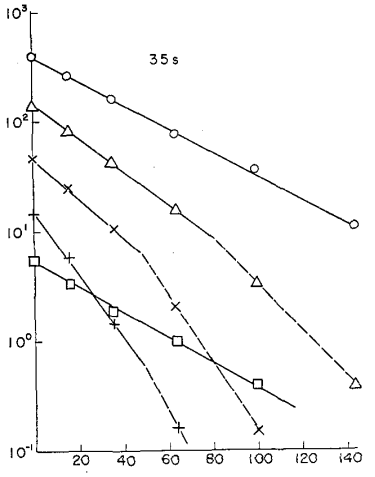

Fig. 3-9.

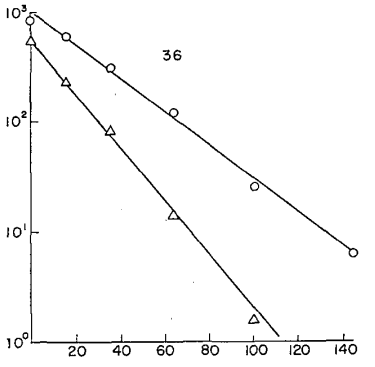

Fig. 3-10.

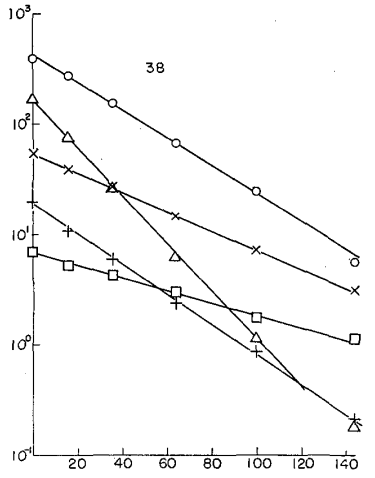

Fig. 3-11.

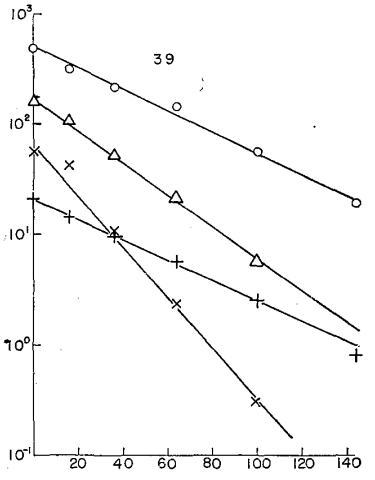

Fig. 3-12.

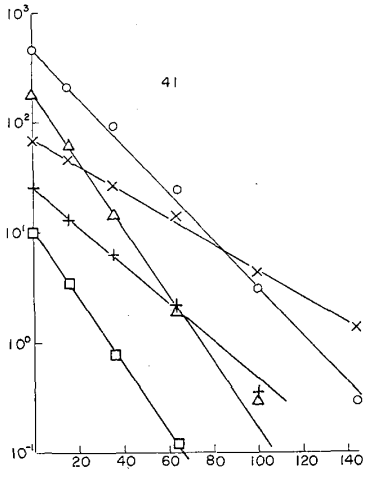

Fig. 3-13.

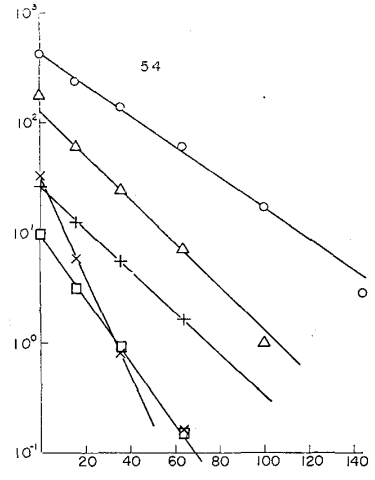

Fig. 3-14.

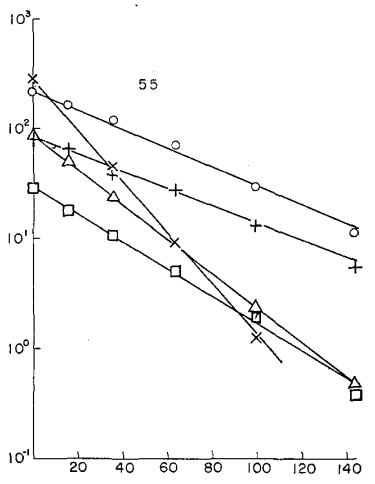

Fig. 3-15.

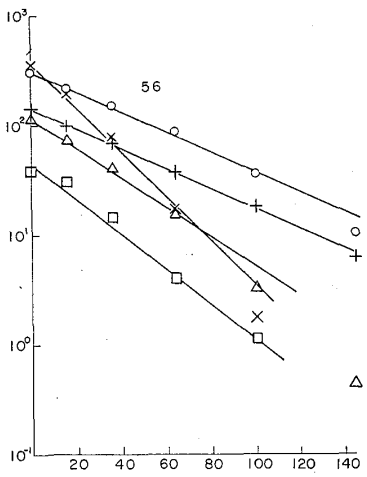

Fig. 3-16.

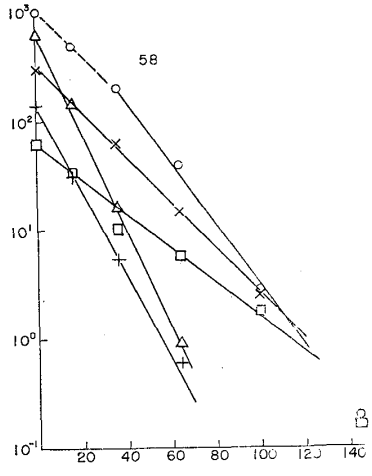

Fig. 3-17.

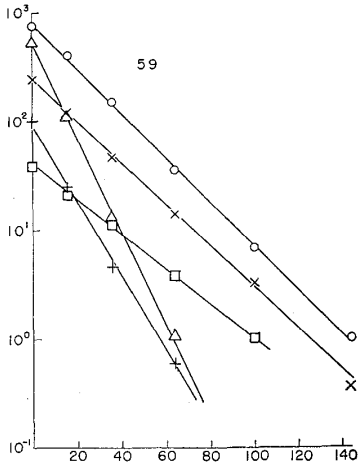

Fig. 3-18.

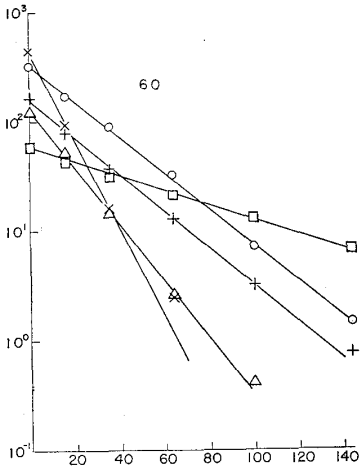

Fig. 3-19.

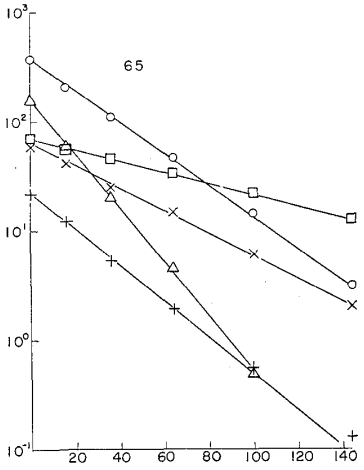

Fig. 3-20.

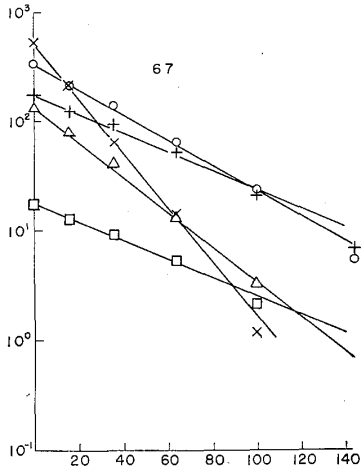

Fig. 3-21.

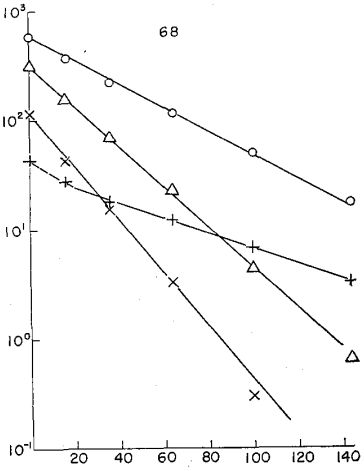

Fig. 3-22.

ing to the above assumption, the radius vector which indicates the position of a puff emitted from the source may be expressed by

$$\tilde{r}(t)=\int_0^t \tilde{s}(t)dt \tag{4}.$$

The angular position φ of the puff which reached at the leeward (radial) distance ρ may be expressed by

$$\varphi(t)=\arg[\tilde{r}_\rho(t)]=\arg\left[\int_0^{t_\rho}\tilde{s}(t)\,dt\right] \tag{5},$$

where t_ρ is calculated by

$$\left|\int_0^{t_\rho}\tilde{s}(t)\,dt\right|=\rho \tag{6}.$$

The emitting time of the source is assumed to be sufficiently large and the sampling of the puff begins at t_1 and ends at $t_2=t_1+T$, then the instantaneous angular position $\varphi(\xi)$ on the are of distance x is given by

$$\varphi(\xi)=\arg\left[\int_{t_1+\xi}^{t_1+\xi+t_\rho}\tilde{s}(t)\,dt\right] \qquad 0\leqq\xi\leqq T \tag{7}$$

It is very difficult to carry out the calculations using eqq. (4) to (7), so we assume further as a first approximation that

$$|\tilde{s}(t)|=\text{constant}=\bar{u},$$

where $\bar{u}$ is the mean wind speed.
Then we can write

$$\tilde{s}(t)=\bar{u}\tilde{\theta}(t),$$

$\tilde{\theta}(t)$ is an angular vector. Furthermore, we assume that the process goes on almost stationarily,

$$\bar{u}\left|\int_{t_1+\xi}^{t_1+\xi+t_x}\tilde{\theta}(t)\,dt\right|=\bar{u}\left|\int_{t_1}^{t_1+t_x}\tilde{\theta}(t)\,dt\right|=x$$

and, as the error which occurs by assuming $\sin\theta=\theta$ is less than 10% even when $\theta=45°$, we obtain that

$$t_x=x/\bar{u},$$

and

$$\varphi(\xi)=\arg\left[\bar{u}\int_{t_1+\xi}^{t_1+\xi+x/u}\tilde{\theta}(t)\,dt\right]=\mathrm{Sin}^{-1}\left[(\bar{u}/x)\int_{t_1+\xi}^{t_1+\xi+x/u}\sin\theta(t)\,dt\right]=\int_{t_1+\xi}^{t_1+\xi+x/u}\theta(t)dt\Big/\frac{x}{\bar{u}} \tag{8}$$

Occurrence frequencies of φ during t_1 to t_2 express the horizontal concentration profiles and eq. (8) indicates that φ can be calculated by taking a moving average of interval $x/\bar{u}$ from the record of the

Fig. 4. Curves of standard deviation (A) or plume width (L) against x.

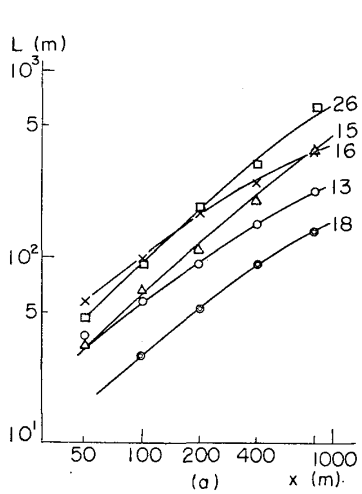

Fig. 4-1.

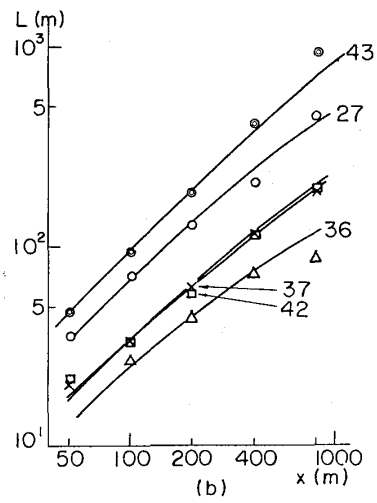

Fig. 4-2.

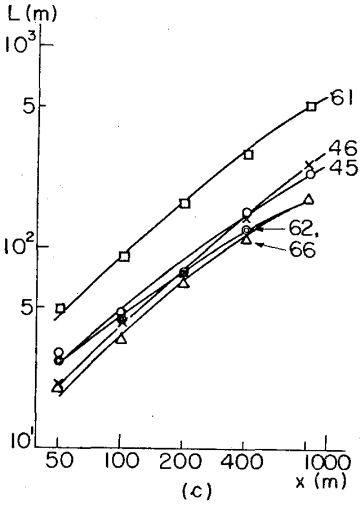

Fig. 4-3.

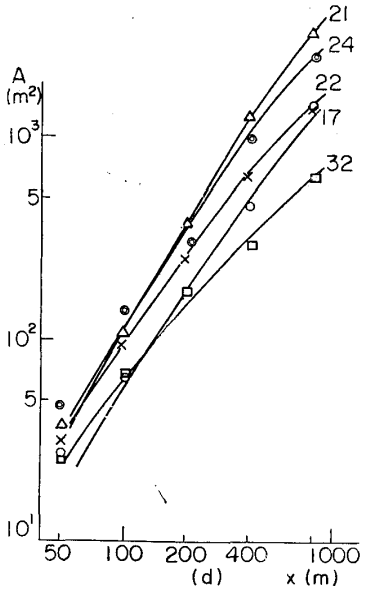

Fig. 4-4.

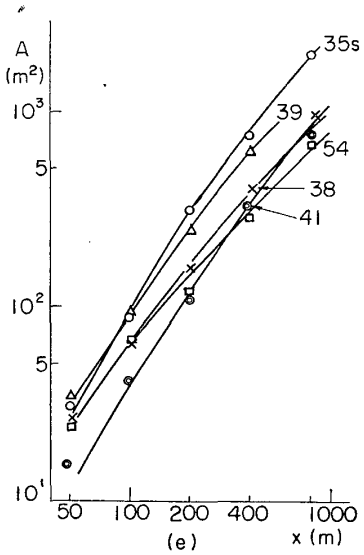

Fig. 4-5.

wind direction at the source.

Standard deviations (A) of profiles or plume widths (L)[3] defined by 1/10 of peak (plateau) concentration are plotted with x in Fig. 4. As well as A, L has the same nature as the standard deviation $\overline{y^2}$. If we assume that

$$R(\xi)=e^{-\alpha\xi} \tag{9}$$

from the well known Taylor's equation,[12]

$$\overline{y^2}=2\overline{v^2}\int_0^t\int_0^\eta R(\xi)\ d\xi d\eta$$

(3) When the profiles showed normal distributions, we determined the values of A; otherwise we determined the values of L.

$$=2\overline{v^2}\int_0^t\int_0^\eta e^{-\alpha\xi}d\xi d\eta=\overline{v^2}\frac{1}{\alpha^2}(\alpha t+e^{-\alpha t}-1), \tag{10}$$

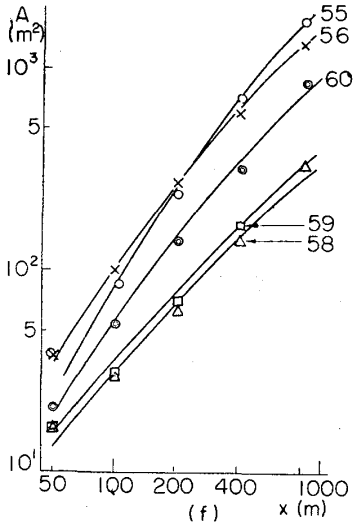

Fig. 4-6.

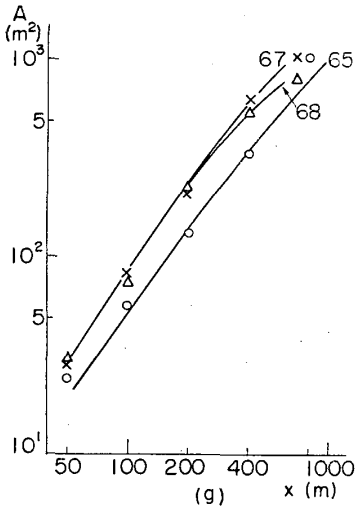

Fig. 4-7.

If we put $t=x/\bar{u}$ and $\varphi_A=\alpha/\bar{u}$, we get

$$\overline{y^2}=2(\overline{v^2}/\alpha^2)(\varphi_A x+e^{-\varphi_A x}-1),$$

and finally

$$L=k\overline{y^2}=q_A(\varphi_A x+e^{-\varphi_A x}-1) \tag{11}$$

where k is a proportionality constant and q_A and φ_A are diffusion parameters. Curves in Fig. 4 are calculated ones with the values of φ_A and q_A determined by the observed data. They will indicate that eq. (11) has an adequate form. The values of φ_A and q_A have a relation, Fig. 5, so only one of them is essential. The values of φ_A and q_A are tabulated in Table 1.

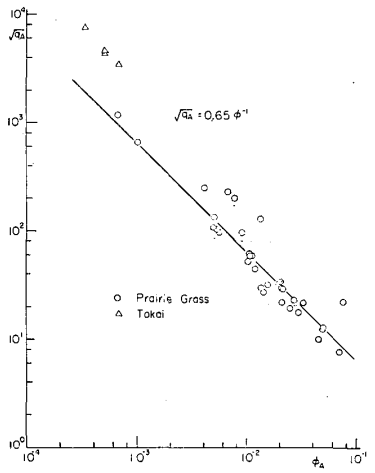

Fig. 5. Relation between q and φ.

Table 1.

Run	φ_A	q_A	$B_{k,100}$	$B_{t,100}$	φ_B	q_B	ζ	$\frac{\partial T}{\partial \log_{10} z} \Big/ \left(\frac{\partial u}{\partial \log_{10} z}\right)^2$	σ_A	1/L
13	9.2^{-3}	8.6^{1}	○0.6	△ 1	1.22^{-1}	5.0^{-2}	5.30	0.52	4.2	0.083
15	6.7^{-4}	1.15^{3}	○4	×	1.22^{-4}	5.6^{4}	−0.276	−1.99	13.2	−0.140
16	1.35^{-2}	1.30^{2}	○10	○150	1.39^{-4}	1.21^{4}	−0.354	−2.68	22.3	−0.140
17	1.59^{-2}	3.2^{1}	○1.75	△ 20	1.39^{-2}	2.8	0.058	0.147	5.3	0.015
18	1.21^{-2}	4.5^{1}	○1.5	△ 20	2.5^{-2}	9.7^{-1}	0.143	0.108	5.9	0.037
21	5.3^{-3}	1.01^{2}	○2	×	1.22^{-2}	3.6	0.022	0.047	7.0	0.005
22	2.17^{-2}	2.95^{1}	○1.8	×	1.0^{-2}	5.1	0.010	0.052	6.4	0.004
24	1.10^{-2}	5.9^{1}	○2	×	9.8^{-3}	5.0	0.007	0.015	6.4	0.004
26	7.7^{-3}	2.00^{2}	○4	×	6.2^{-3}	2.4^{1}	−0.065	−0.405	11.9	−0.026
27	4.1^{-3}	2.50^{2}	○3	×	4.7^{-3}	2.85^{1}	−0.067	−0.371	11.4	−0.024
32	5.0^{-2}	1.25^{1}	△0.5	△ 0.5	3.7^{-2}	2.2^{-1}	0.450	0.247	4.1	0.099
35_s	1.04^{-2}	5.2^{1}	△2	○ 20	1.64^{-2}	2.35	0.029	0.021	5.6	0.014
36	5.0^{-2}	1.3^{1}	○0.7	△ 5	5.0^{-2}	3.4^{-1}	0.688	0.078	6.3	0.077
37	5.6^{-3}	9.8^{1}	○2	△ 30	1.85^{-2}	2.02	0.026	0.030	6.1	0.007
38	1.39^{-2}	3.0^{1}	△1.5	×	1.14^{-2}	3.3	0.022	0.039	6.1	0.007
39	3.3^{-2}	2.2^{1}	△1.5	△ 40	1.32^{-2}	2.8	0.300	0.063	12.0	0.114
41	1.45^{-2}	2.75^{1}	△1.0	○ 20	2.0^{-2}	1.08	0.058	0.039	4.9	0.015
42	5.0^{-3}	1.08^{1}	○2	△ 20	1.47^{-2}	2.8	0.015	0.070	6.5	0.008
43	1.0^{-3}	6.4^{2}	△5	×	2.56^{-3}	1.39^{2}	−0.135	−0.920	14.4	−0.045
45	9.1^{-3}	8.8^{1}	○2.5	×	8.3^{-3}	8.8	−0.021	−0.125	9.4	−0.008
46	2.0^{-3}	3.30^{2}	○2	×	1.37^{-2}	2.8	0.021	0.074	8.7	0.010
54	3.0^{-2}	1.8^{1}	○1.5	△ 20	1.89^{-2}	1.52	0.055	0.050	5.7	0.021
55	2.0^{-2}	3.3^{1}	○2	×	1.18^{-2}	4.1	0.017	0.066	5.6	0.005
56	2.17^{-2}	2.95^{1}	△2	○ 30	1.35^{-2}	4.0	0.026	0.058	8.2	0.010
58	7.0^{-2}	7.7	○0.4	○ 5	5.3^{-2}	1.4^{-1}	0.93	0.140	5.4	0.091
59	4.5^{-2}	1.0^{1}	○1.5	△ 5	3.3^{-2}	6.8^{-1}	0.253	0.132	6.9	0.077
60	2.12^{-2}	2.2^{1}	○1.5	×	1.39^{-2}	2.3	0.040	0.063	6.1	0.018
61	6.7^{-3}	2.30^{2}	○1.7	×	6.7^{-3}	9.0	−0.042	−0.84	11.6	−0.019
62	1.08^{-2}	6.1^{1}	○3	×	6.5^{-3}	1.65^{1}	−0.062	−1.6	8.2	−0.020
65	2.5^{-2}	1.95^{1}	○1.5	×	2.0^{-2}	1.40	0.048	0.037	9.0	0.015
66	1.10^{-2}	5.9^{1}	○1.0	○ 1.0	2.5^{-2}	7.8^{-1}	0.152	0.106	12.8	0.040
67	2.77^{-2}	2.33^{1}	○1.5	△ 20	1.56^{-2}	1.95	0.021	0.088	13.2	0.010
68	2.77^{-2}	2.30^{1}	○1.0	×	2.20^{-2}	9.2^{-1}	0.108	0.110	16.3	0.048

φ_A and φ_B in m^{-1}
q_A and q_B in m^2
$B_{k,100}$ and $B_{t,100}$ in m^2
$\frac{\partial T}{\partial \log_{10} z} \Big/ \left(\frac{\partial u}{\partial \log_{10} z}\right)^2$ in $deg.sec^2/m^2$
σ_A in deg.
1/L in m^{-1}
e. g. 9.2^{-2} means 9.2×10^{-3}.

Vertical concentration profiles

The vertical concentration profiles were observed only at five positions at a distance 100 m from the source. The observed results were analysed and the values of B in eq. (3) were determined. (Fig. 6)

As the source was a point source and the distance 100 m was rather short, the plume width was not so wide; therefore, the meandering of wind, which was not always uniform in height during sampling period, might effect remarkably on the vertical profiles, so all data of the five positions were not always reasonable, and we analysed only some of them.

We also analysed the results by the Sutton's eq. (1). However, many runs were unable to determine the values of B. In Table 1, B_k and B_t denote the values of B obtained by eq. (3) and by eq. (1) respectively; and the marks ○ mean that the degree of agreement

Fig. 6. Curves of log χ against z.
(Tower No.: ○: 1, △: 2, ×: 3, □: 4, +: 5, ●: 6)

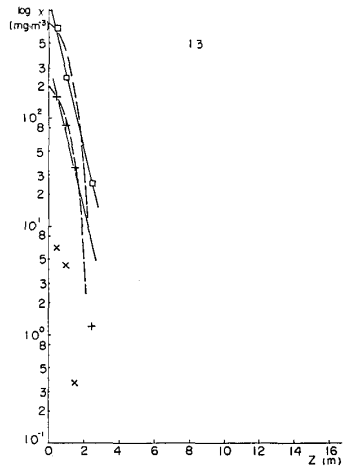

Fig. 6-1.

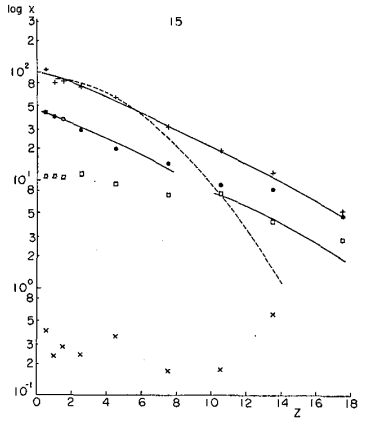

Fig. 6-2.

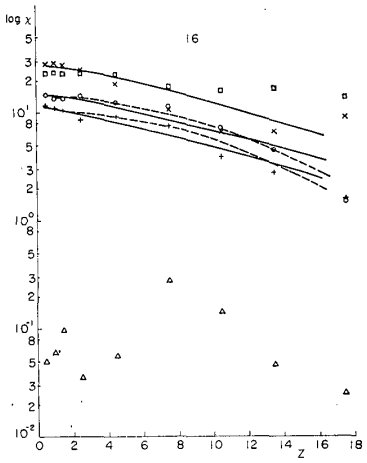

Fig. 6-3.

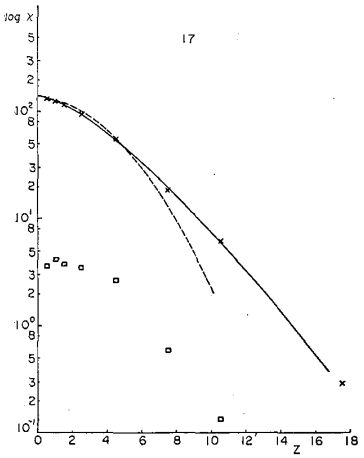

Fig. 6-4.

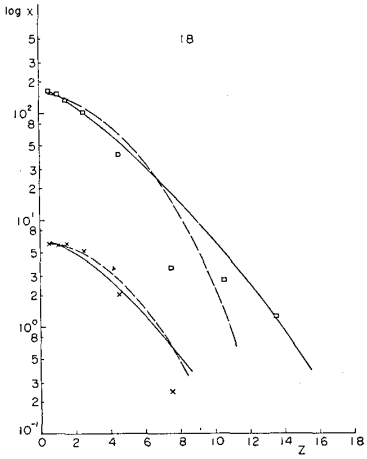

Fig. 6-5.

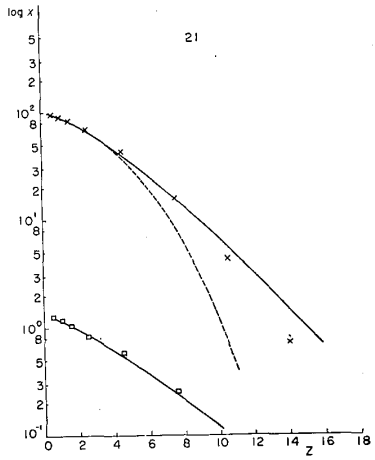

Fig. 6-6.

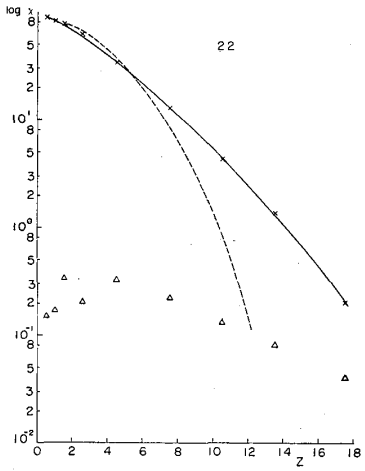

Fig. 6-7.

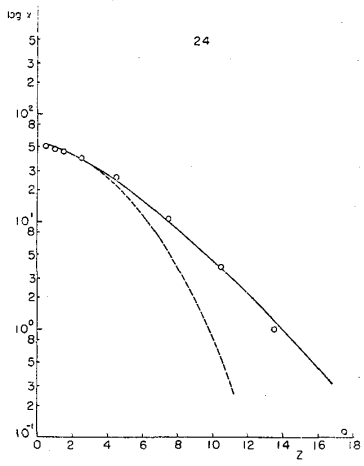

Fig. 6-8.

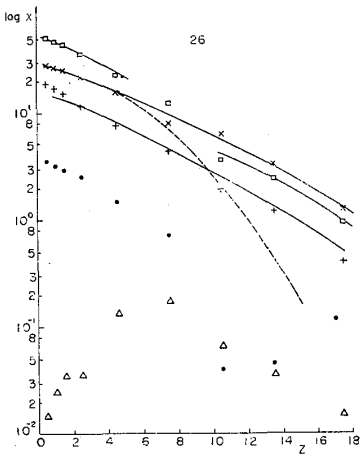

Fig. 6-9.

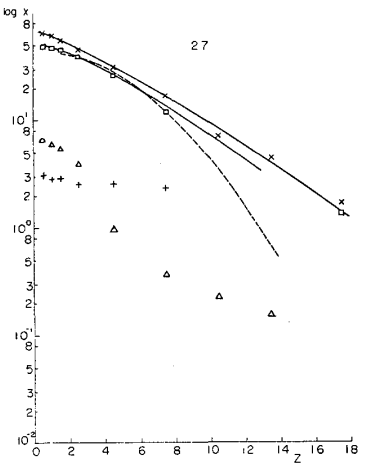

Fig. 6-10.

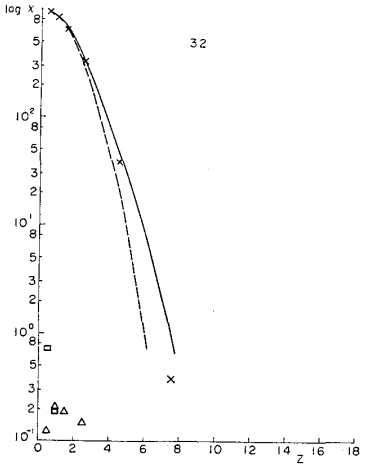

Fig. 6-11.

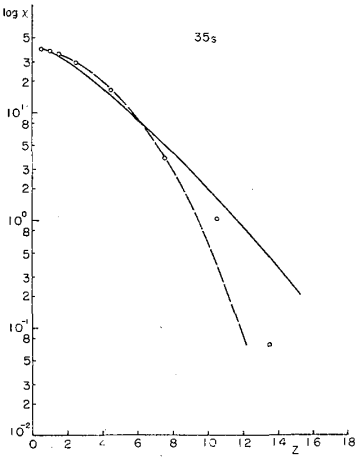

Fig. 6-12.

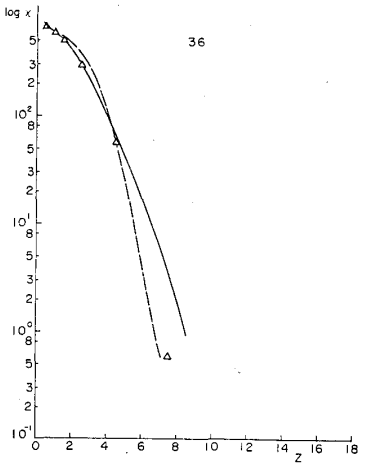

Fig. 6-13.

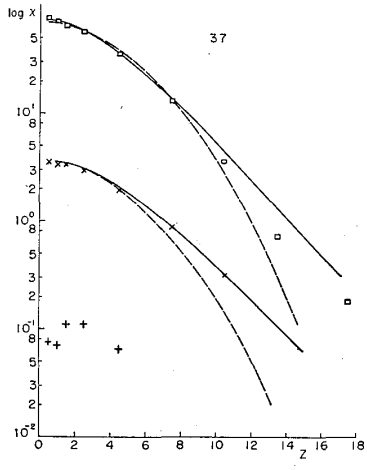

Fig. 6-14.

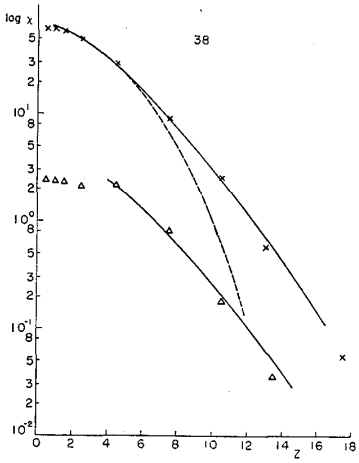

Fig. 6-15.

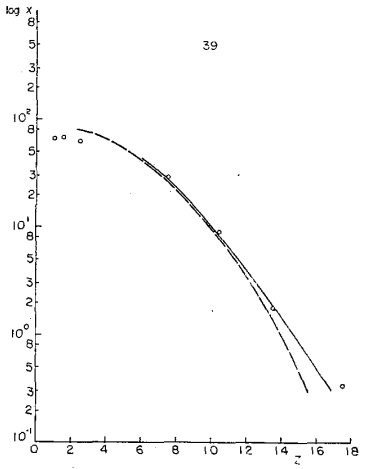

Fig. 6-16.

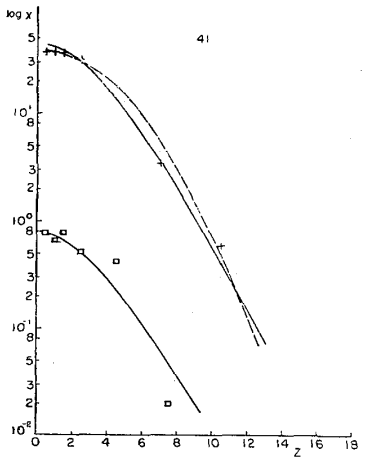

Fig. 6-17.

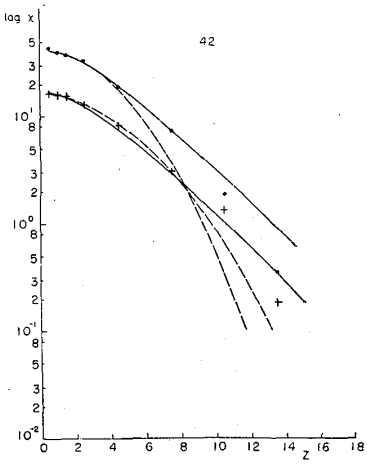

Fig. 6-18.

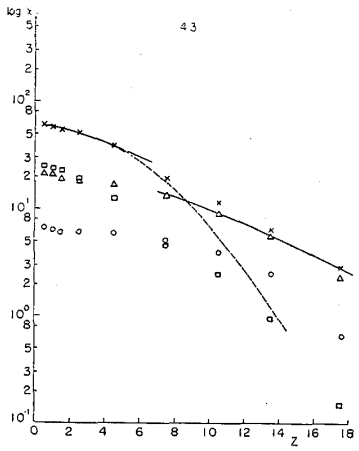

Fig. 6-19.

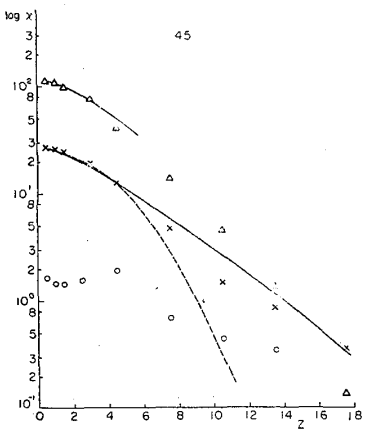

Fig. 6-20.

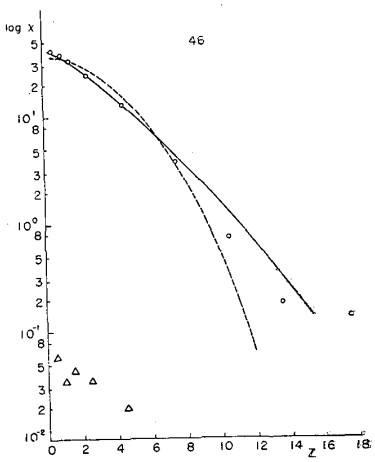

Fig. 6-21.

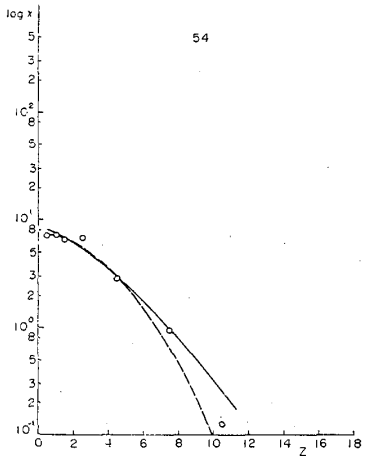

Fig. 6-22.

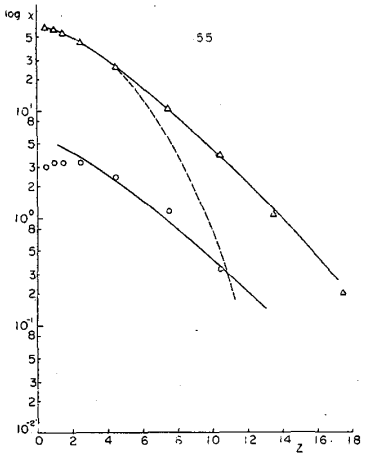

Fig. 6-23.

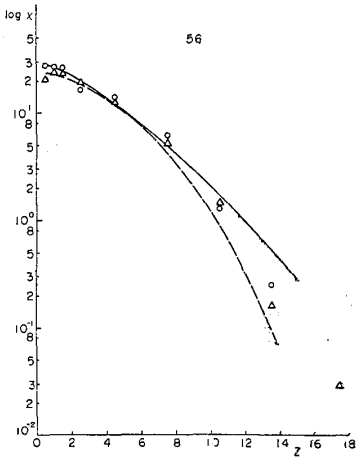

Fig. 6-24.

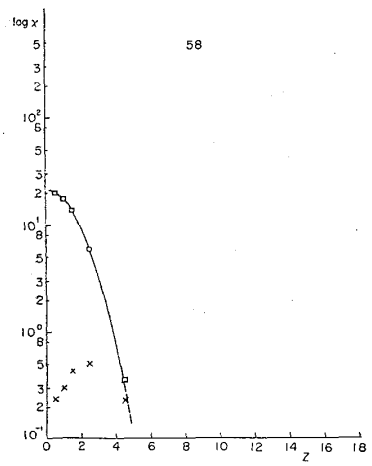

Fig. 6-25.

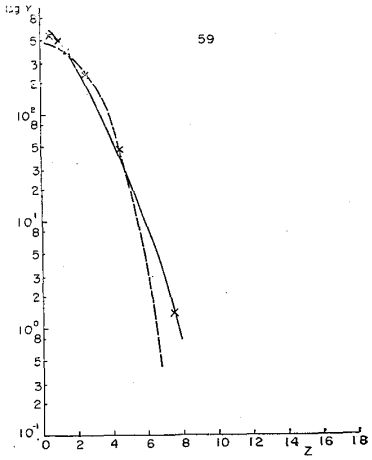

Fig. 6-26.

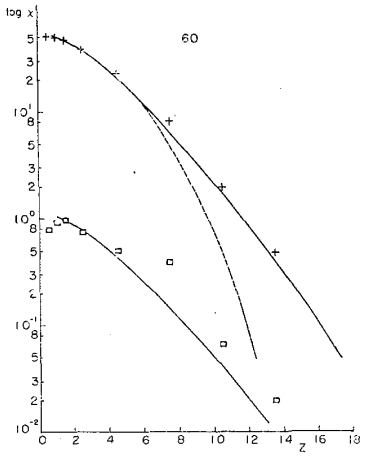

Fig. 6-27.

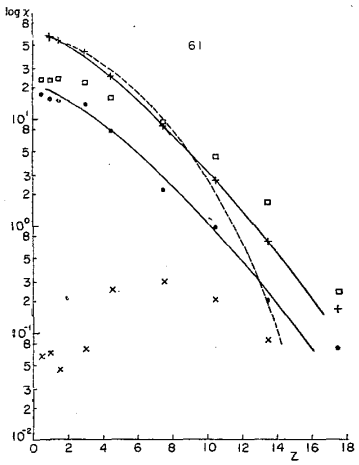

Fig. 6-28.

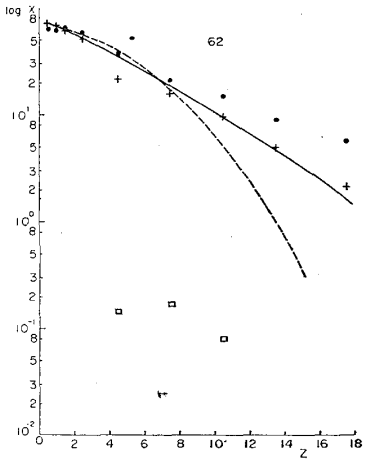

Fig. 6-29.

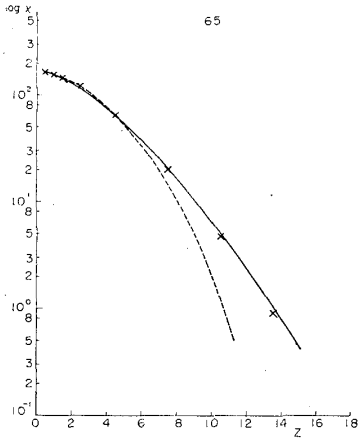

Fig. 6-30.

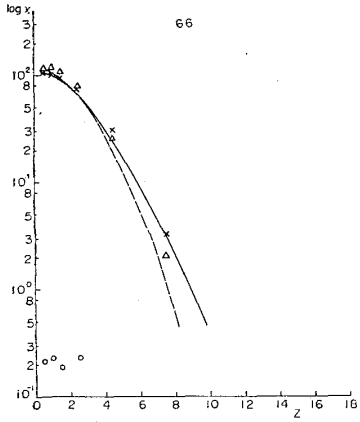

Fig. 6-31.

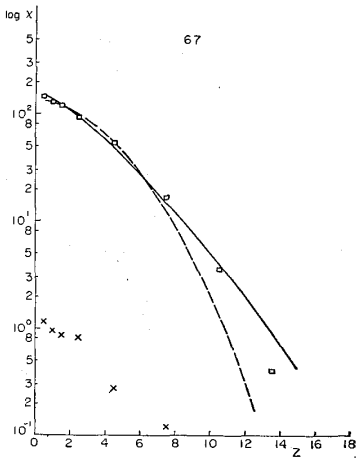

Fig. 6-32.

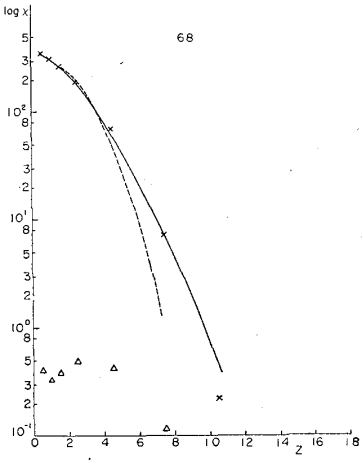

Fig. 6-33.

is good, and the marks △ and × mean that it is tolerable and poor respectively.

On the other hand, we consider χ_{CIC}, which is defined by

$$\chi_{CIC}=\int_{-\infty}^{\infty}\chi\,dy \tag{12}$$

This quantity is expressed by

$$\chi_{CIC}=\frac{Q}{u}\frac{1}{\sqrt{\pi B}}\left(e^{-\frac{(h+z)^2}{B}}+e^{-\frac{(h-z)^2}{B}}\right) \quad \text{(Sutton)} \tag{13}$$

$$=\frac{Q}{u}\frac{1}{B}e^{-\frac{h+z}{B}}J_0\left(i\frac{2\sqrt{hz}}{B}\right) \quad \text{(Author)} \tag{14}$$

which indicate that χ_{CIC} is determined only by vertical diffusion parameters. We calculated the values of χ_{CIC} from the observed data. Marks in Fig. 7 show the results of observation. With the values of B at $x=100$ m (B_{100}) and the observed results of χ_{CIC}, we could evalute the values of B at each distance. (Fig. 8) The way of determination of B by using the data Q, u and χ_{CIC} is not adequate, because the

Fig. 7. Curves of χ against x.

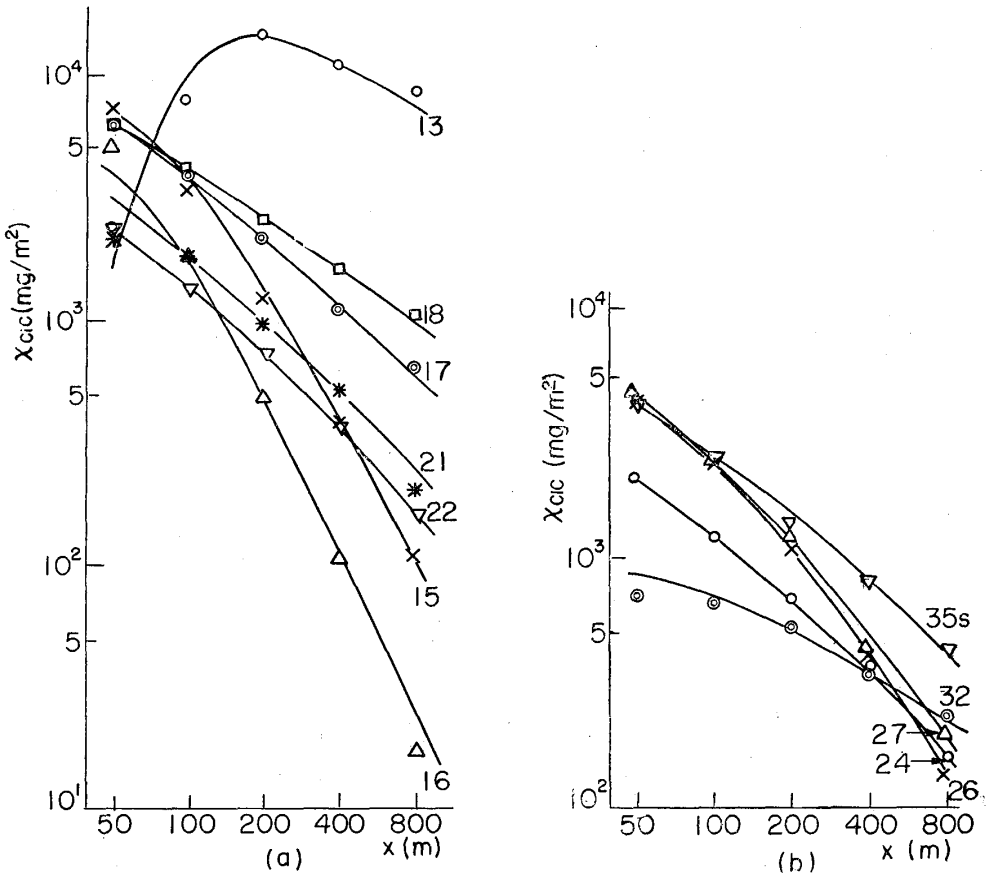

Fig. 7-1. Fig. 7-2.

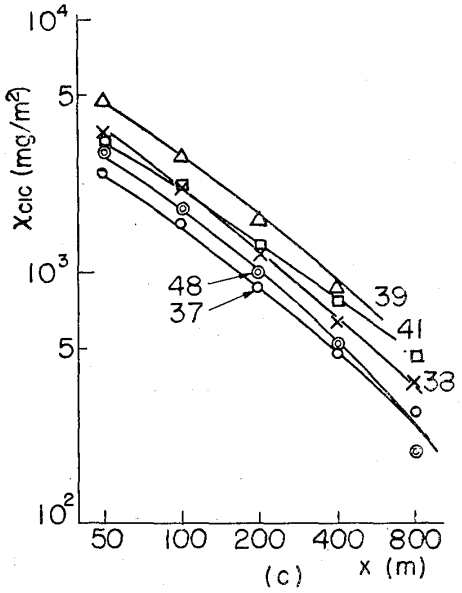

Fig. 7-3.

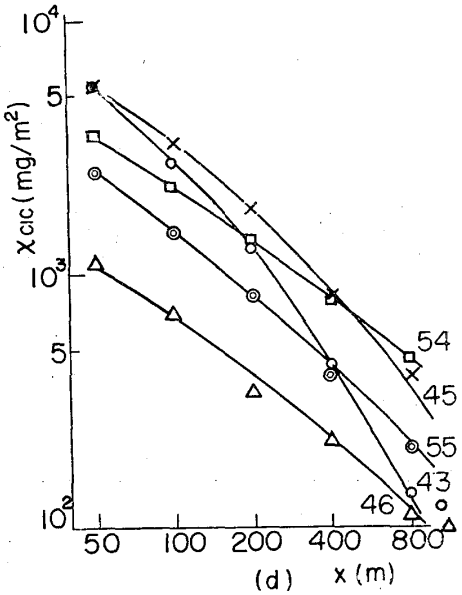

Fig. 7-4.

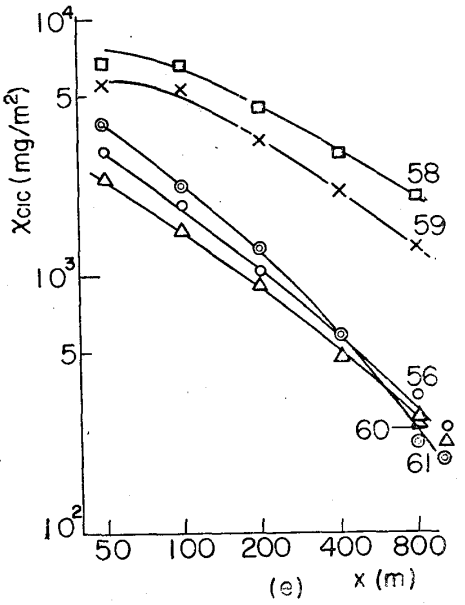

Fig. 7-5.

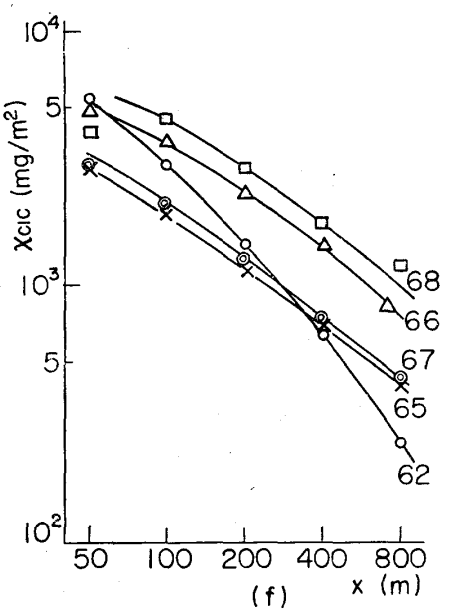

Fig. 7-6.

errors in Q and u often make unable to determine the values of B.

Now we consider the nature of B in eq. (3) or (14). When the source is so high that we can assume that $h/B \ll 1$, the essential part of eq. (14) becomes

Fig. 8. Curves of B against x.

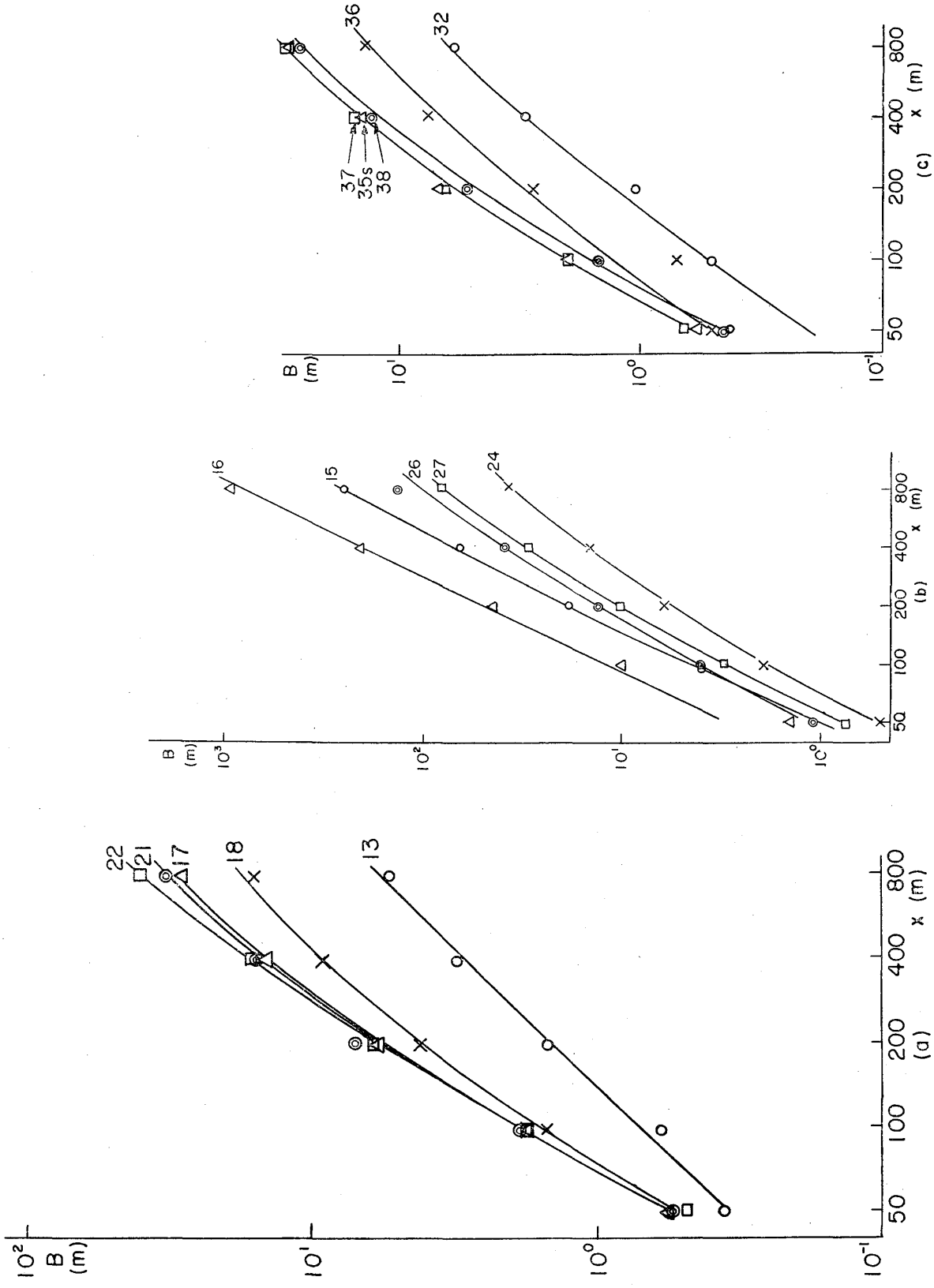

Fig. 8-1.

Fig. 8-2.

Fig. 8-3.

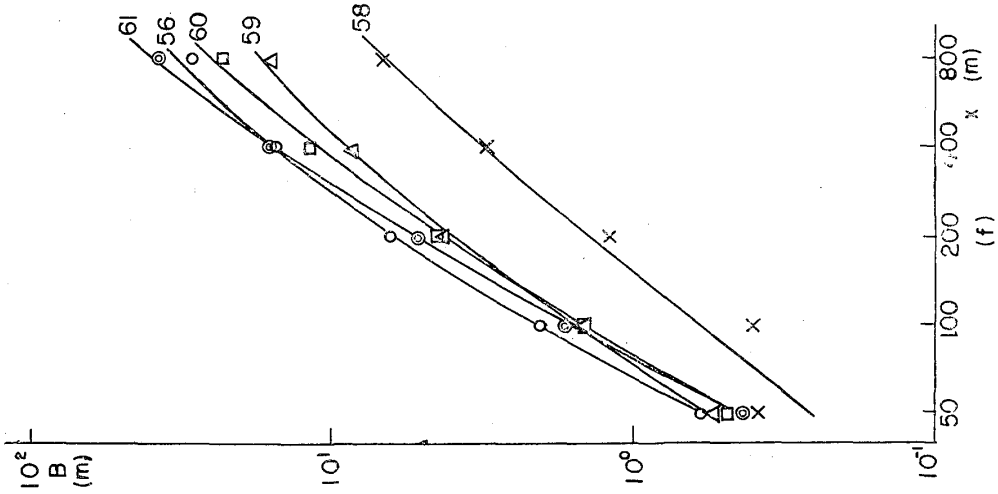

Fig. 8-6.

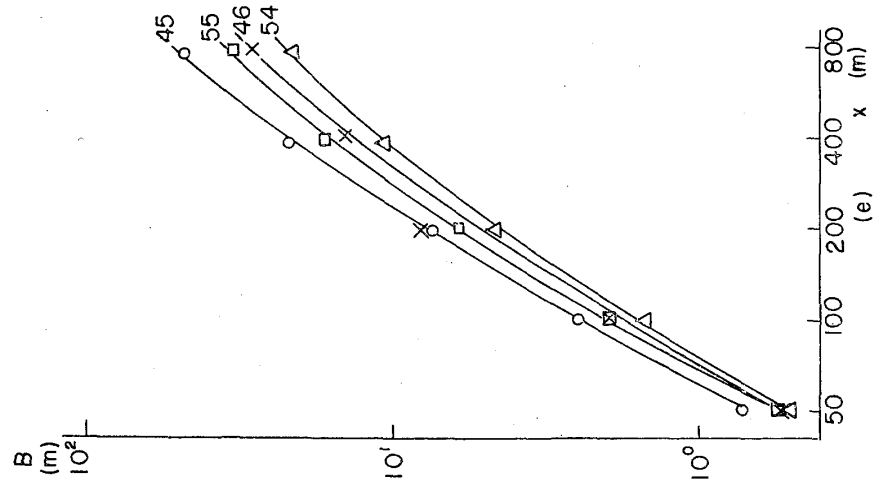

Fig. 8-5.

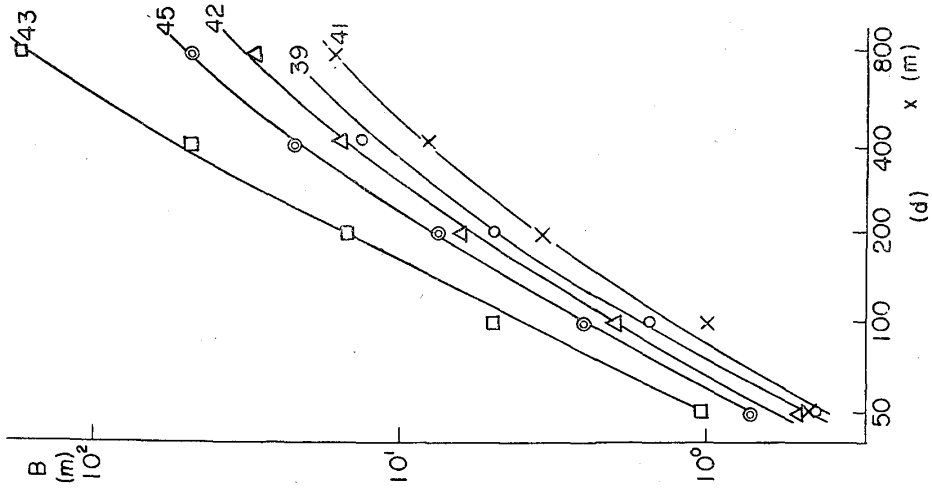

Fig. 8-4.

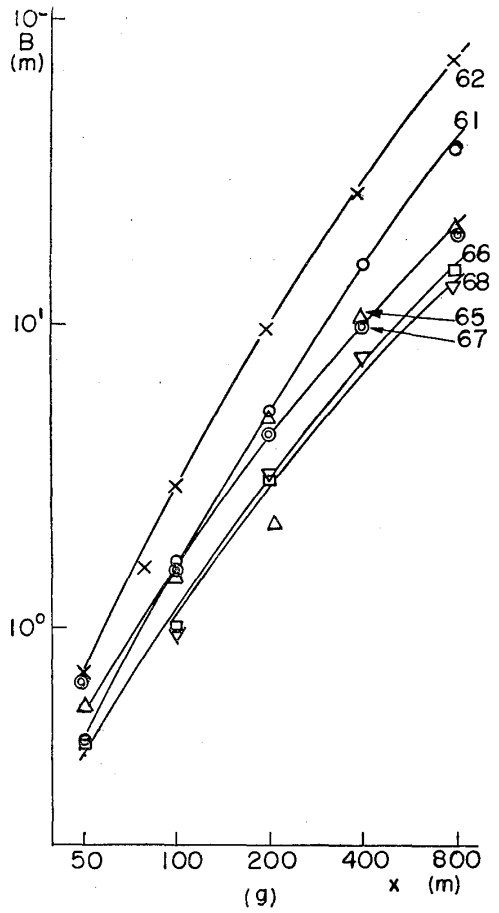

Fig. 8-7.

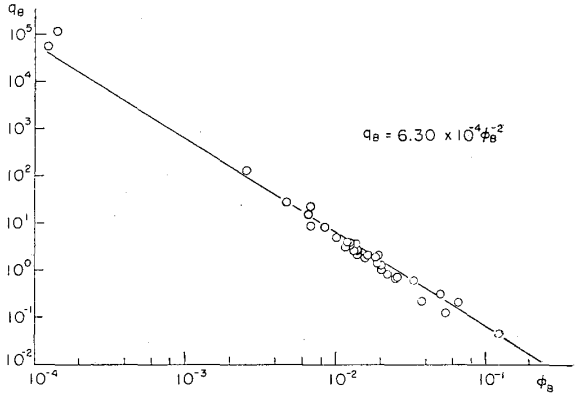

Fig. 9. Relation between q_B and φ_B.

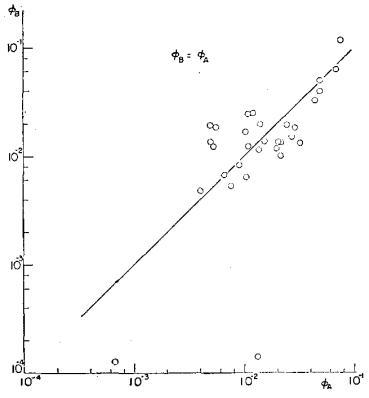

Fig. 10. Relation between φ_B and φ_A.

$$\frac{e^{-\frac{h+z}{B}} J_0\left(i\frac{2\sqrt{hz}}{B}\right)}{B} = \frac{1}{B} e^{-\frac{h}{B}\left(1+\frac{z}{h}\right)} J_0\left(i\frac{2h}{B}\sqrt{\frac{z}{h}}\right)$$

$$\sim \frac{1}{B} e^{-\frac{h}{B}\left(1+\frac{z}{h}\right)} \frac{e^{\frac{2h}{B}\sqrt{\frac{z}{h}}}}{\sqrt{2\pi\frac{2h}{B}\sqrt{\frac{z}{h}}}} = \frac{e^{-\frac{h}{B}\left(1-\sqrt{\frac{z}{h}}\right)}}{\sqrt{4\pi Bh\sqrt{\frac{z}{h}}}} \tag{15}$$

If we put $z=h+\varepsilon$ and $z/h=1+\varepsilon/h=1+\phi$, eq. (15) becomes

$$\frac{e^{-\frac{h}{B}\frac{\phi^2}{4}}}{\sqrt{4\pi Bh\left(1+\frac{\phi}{2}\right)}} = \frac{e^{-\frac{\varepsilon^2}{4Bh}}}{\sqrt{4\pi Bh}} \tag{16}$$

Eq. (16) shows a normal distribution, as it is expected, and that B is proportional to the standard deviation. Hence, similary to L, we can assume that B takes the form of

$$B = q_B(\varphi_B x + e^{-\varphi_B x} - 1) \tag{17}$$

Using eq. (17), we analysed the observational data and determined the values of q_B and φ_B (Table 1). Curves in Fig. 8 are calculated with these values and, as before, they indicate that eq. (17) has an adequate form. Using these values of q_B and φ_B, we calculated conversely the values of χ_{CIC} for each distance, and they are shown as curves in Fig. 7. They may indicate that the eq. (14) express the observed results fairly good over the whole field of experiments. q_B and φ_B have a relation, Fig. 9, so only one of them is essential. Relation between φ_B and φ_A and that between q_B and q_A, are shown in Figs. 10 and 11.

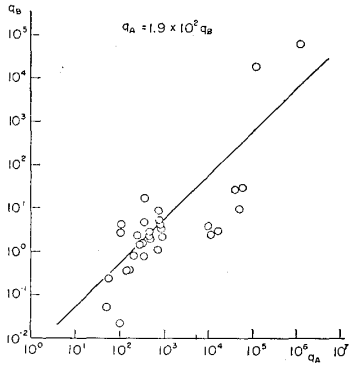

Fig. 11. Relation between q_B and q_A.

Diffusion parameters and meteorological ones

As the meteorological parameters, Richardson number R_i, stability ratio SR, stability length SL and standard deviation of azumuthal angle of wind direction σ_A (Cramer)[8] have hitherto been considered. Concerning the analysis of micrometeorological data, some of them were fairly effective, but for the analysis of diffusion data, they are not always so effective. About these circumstances we shall discuss in another chance. Among them, SR was more suitable for the analysis of diffusion data than others, but, as this is defined by temperature and wind speed at three heights which are chosen occasionally, it is difficult to reduce the results to other series of experiments.

On the other hand, almost of all runs in Project Prairie Grass, the vertical profiles of temperature T and wind speed u in the vertical region in which the diffusion phenomena were effective were expressed approximately by logarithmic laws:

$$T = F \log (z/z_0) \tag{18}$$

$$u = \frac{v_*}{\kappa} \log (z/z_0) \tag{19}$$

where v_*, κ, z_0 and F are constants determined by observations. (Fig.

12). There can be some nondimensional quantities which are independent of height. However, it is noticed both theoretically and experimentally that, as for temperature, its gradient should be taken into account; and as for wind speed, the values themselves should be adopted, because the values of wind speeds are more effective than its

Fig. 12. Vertical profiles of temperature and wind velocity.
(○: temperature, °C; △: wind speed, cm/sec).

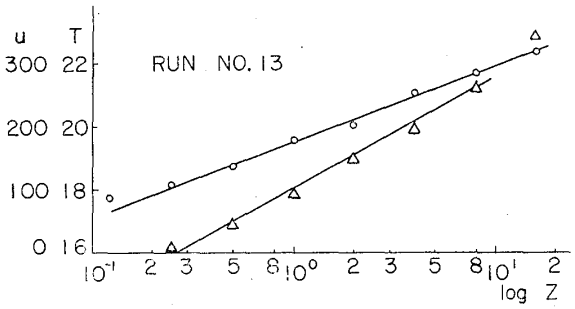

Fig. 12-1.

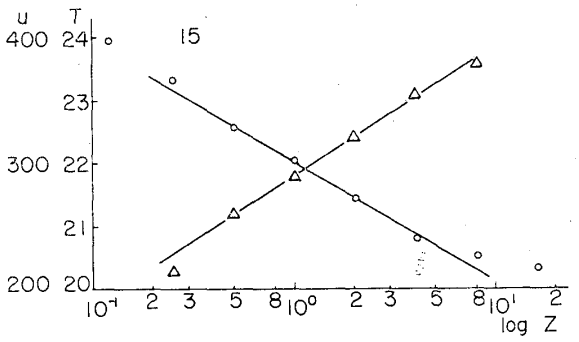

Fig. 12-2.

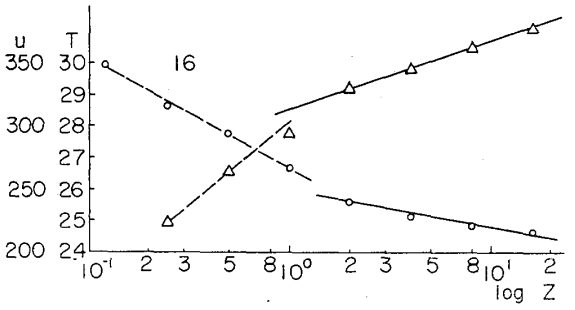

Fig. 12-3.

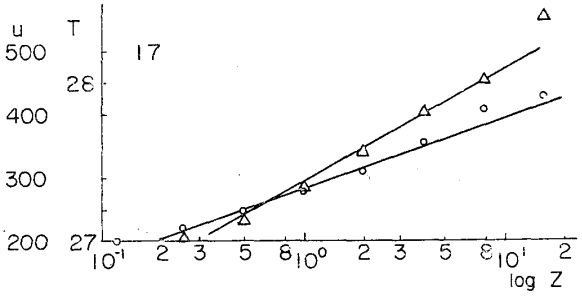

Fig. 12-4.

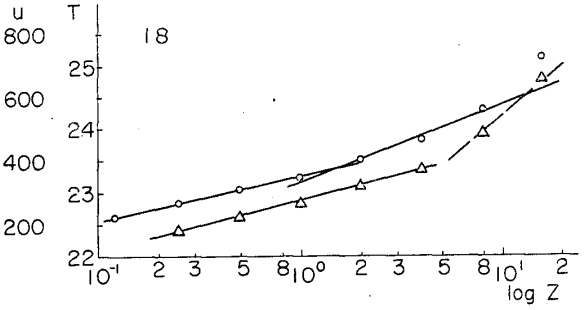

Fig. 12-5.

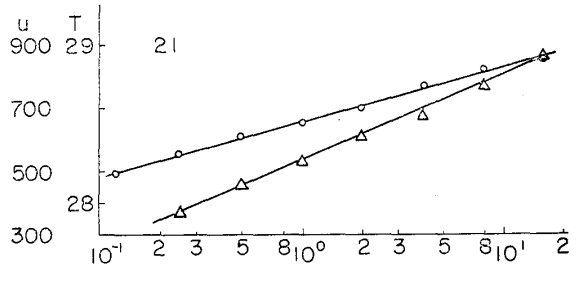

Fig. 12-6.

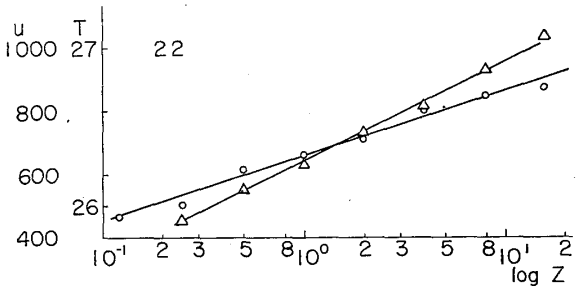

Fig. 12-7.

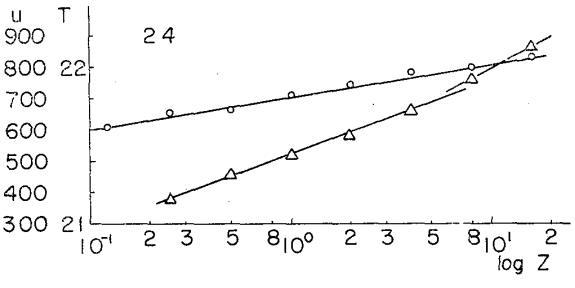

Fig. 12-8.

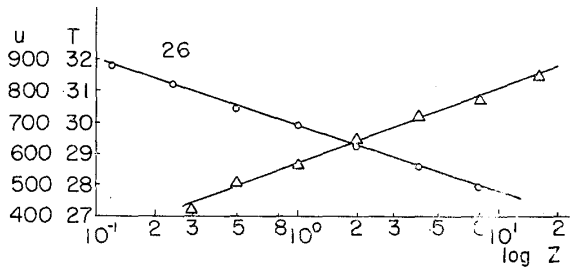

Fig. 12-9.

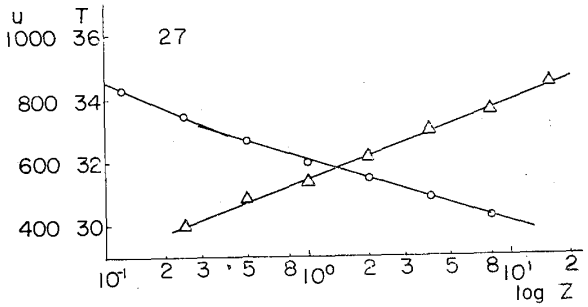

Fig. 12-10.

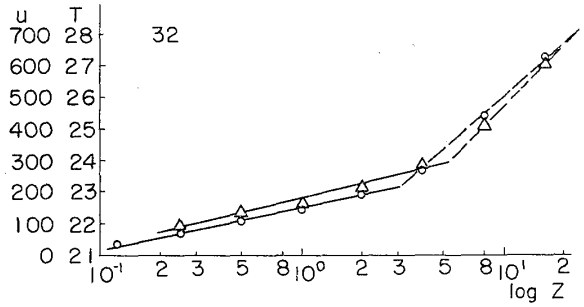

Fig. 12-11.

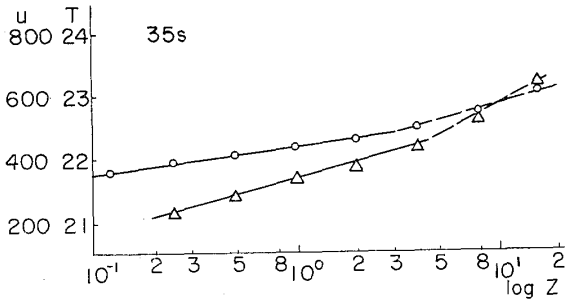

Fig. 12-12.

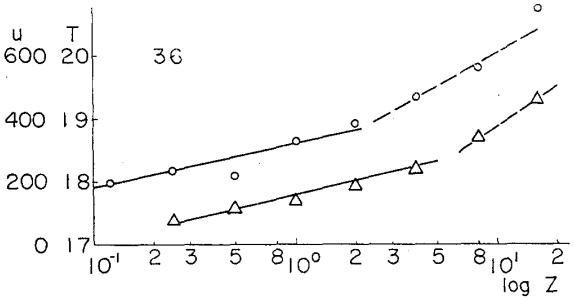

Fig. 12-13.

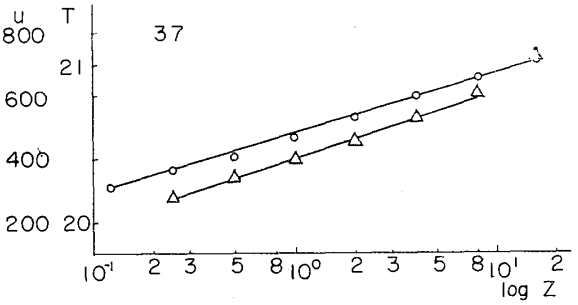

Fig. 12-14.

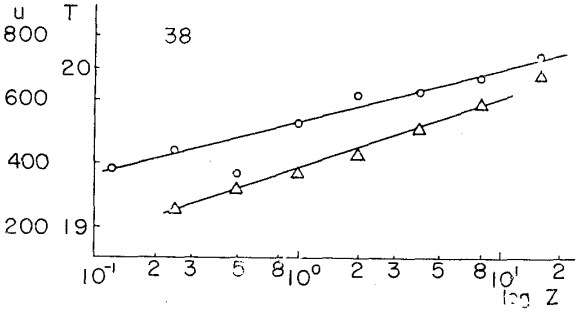

Fig. 12-15.

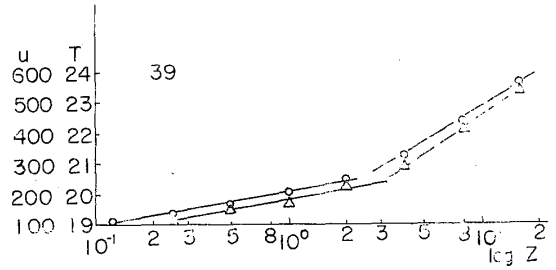

Fig. 12-16.

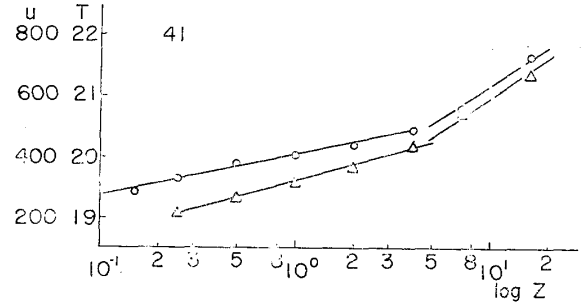

Fig. 12-17.

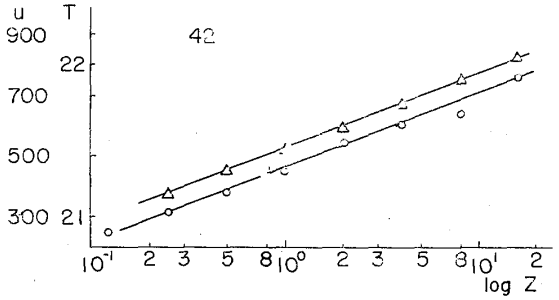

Fig. 12-18.

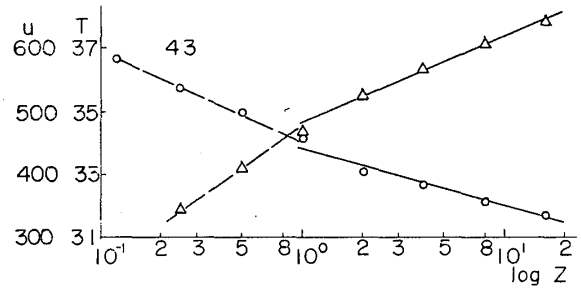

Fig. 12-19.

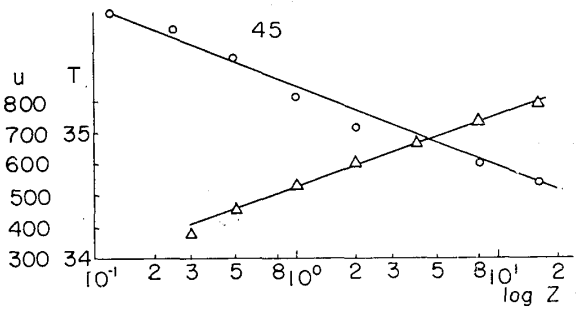

Fig. 12-20.

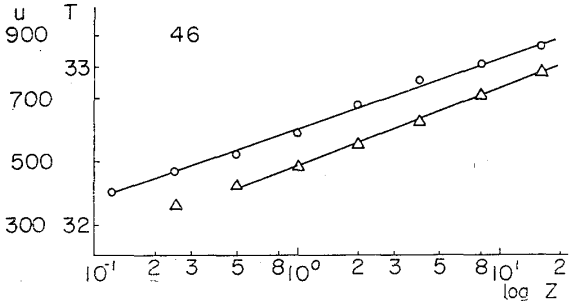

Fig. 12-21.

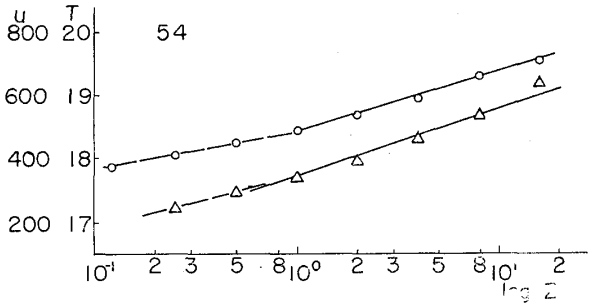

Fig. 12-22.

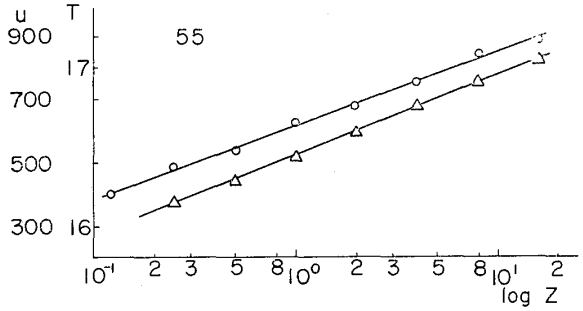

Fig. 12-23.

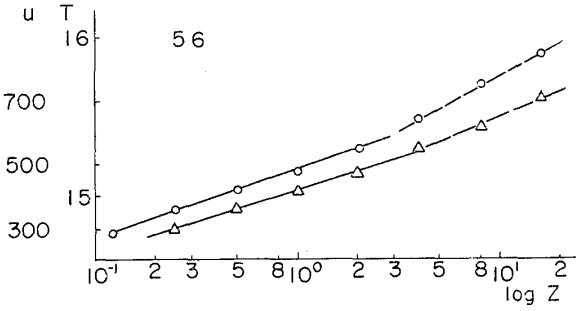

Fig. 12-24.

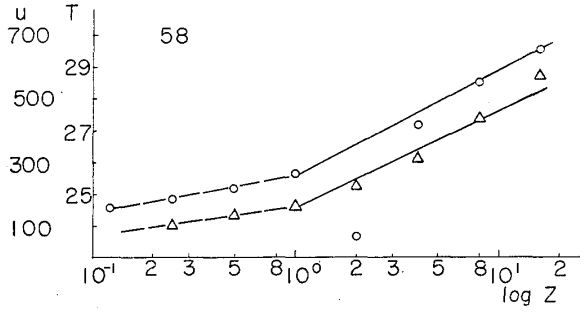

Fig. 12-25.

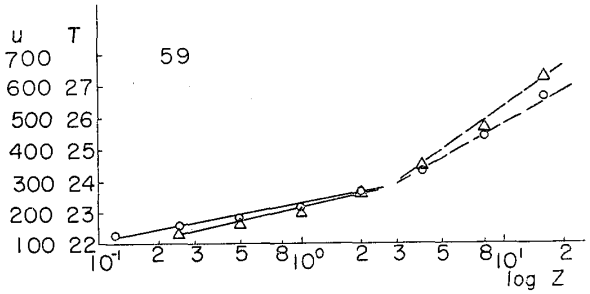

Fig. 12-26.

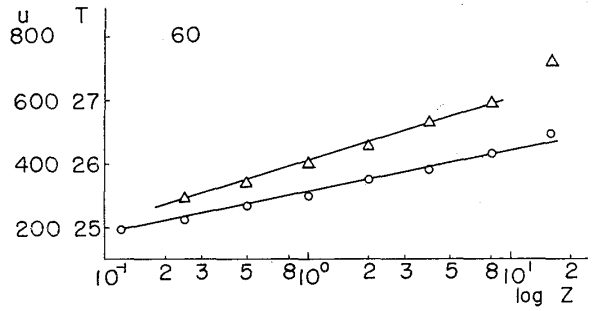

Fig. 12-27.

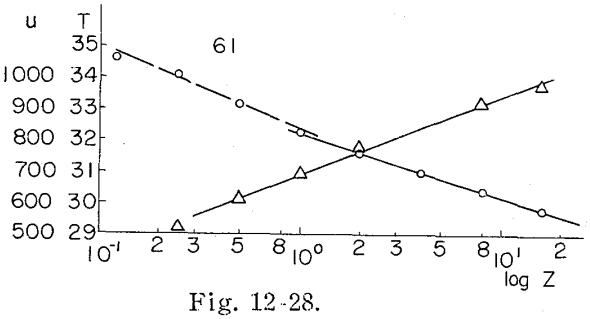

Fig. 12-28.

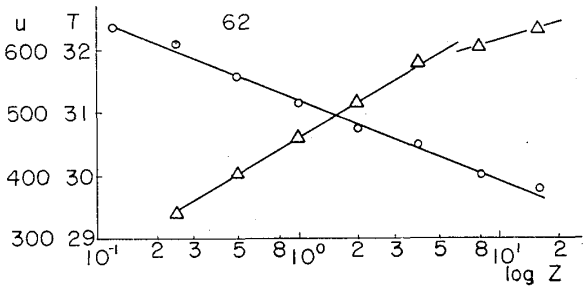

Fig. 12-29.

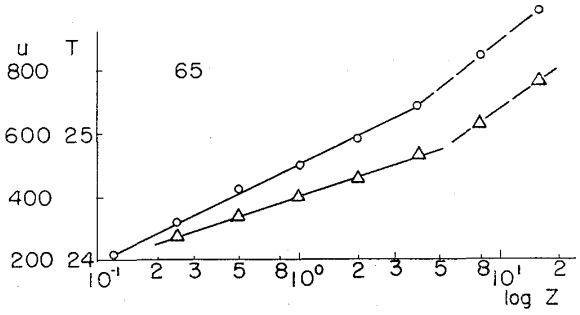

Fig. 12-30.

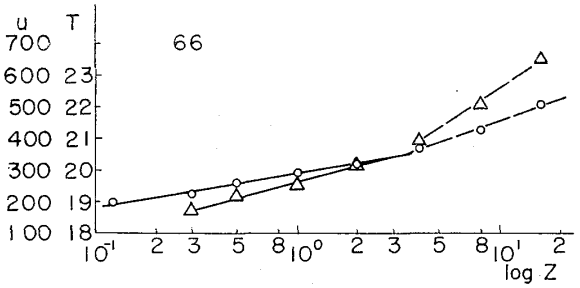

Fig. 12-31.

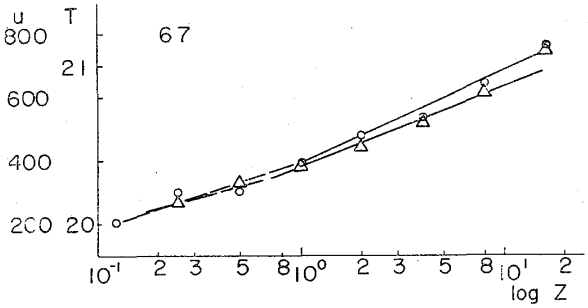

Fig. 12-32.

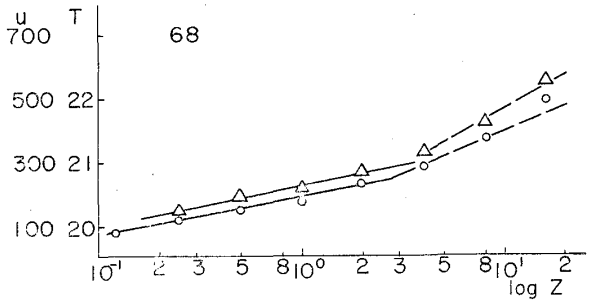

Fig. 12-33.

gradient. So we adopted next parameter:

$$\zeta = \frac{\partial T}{\partial \log_{10} z} \Big/ \left(\frac{v_*}{\kappa} \log_{10} z_0 \right)^2 \tag{20}$$

The values of this parameter can be determined from the data of observations, with few ambiguities at most (Table 1).

The relations between diffusion parameters (φ_A, q_A, φ_B and q_B) and ζ are shown in Figs. 13~16. The points in these figures arrange more closely on respective curves than those plotted against with other parameters:- for example as shown in Fig. 17, in which the parameter is $\dfrac{\partial T}{\partial \log_{10} z} \Big/ \left(\dfrac{\partial u}{\partial \log_{10} z} \right)^2$.[4]

By the way, we examined the adequateness of using σ_A^2 (Table 1).

(4) This quantity is nearly proportional to *Ri*.

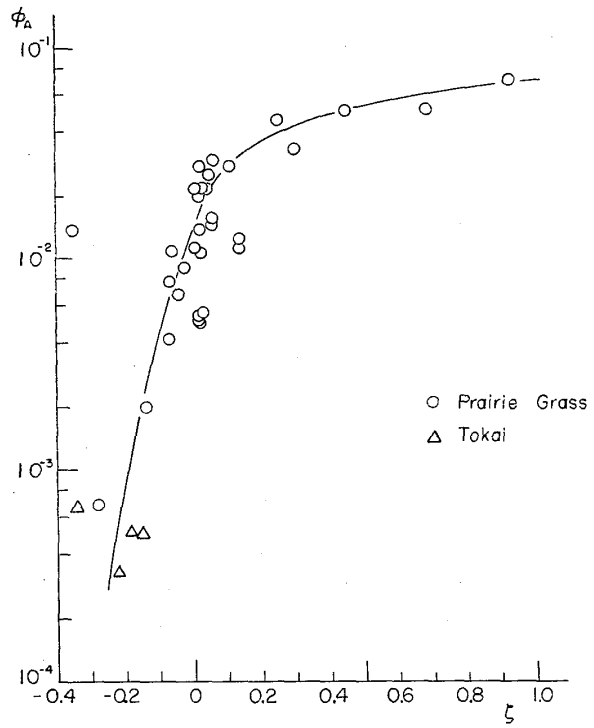

Fig. 13. Relation between φ_A and ζ.

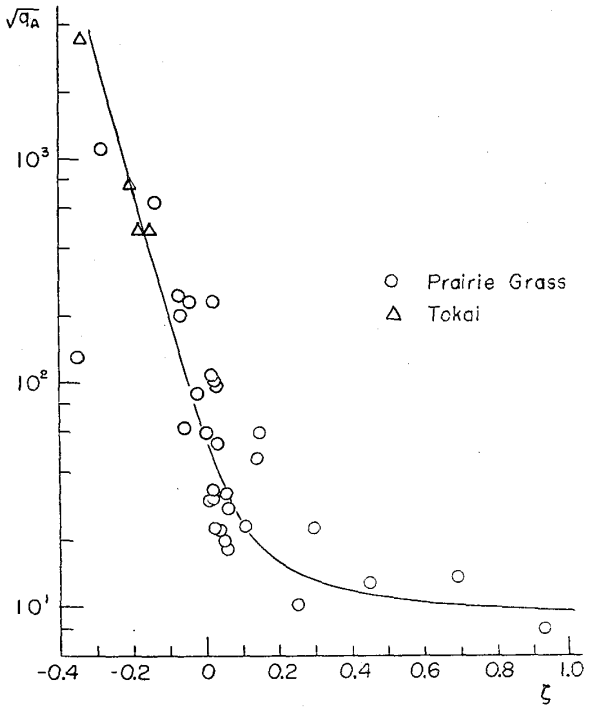

Fig. 14. Relation between $\sqrt{q_A}$ and ζ.

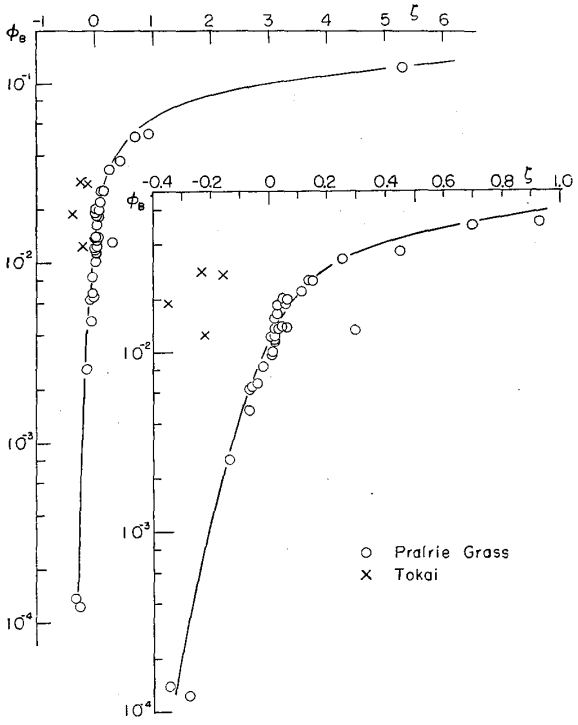

Fig. 15. Relation between φ_B and ζ.

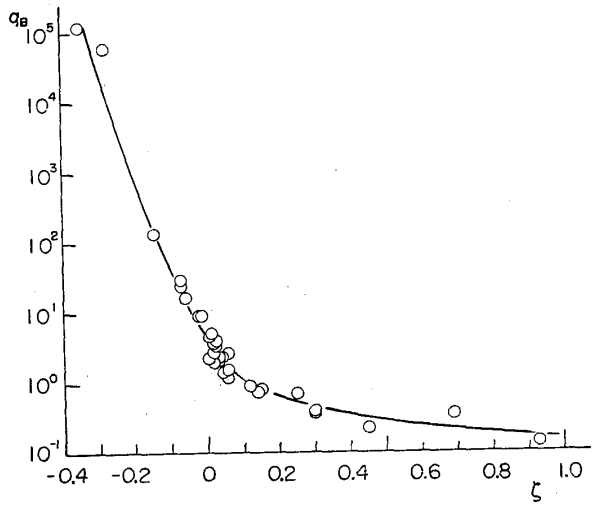

Fig. 16. Relation between q_B and ζ.

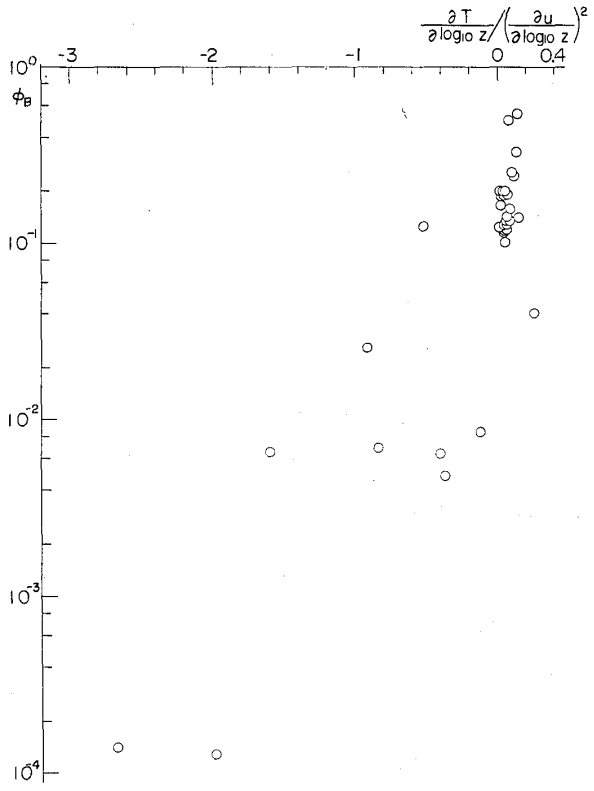

Fig. 17. Relation between q_B and $\dfrac{\partial T}{\partial \log_{10} z} \Big/ \left(\dfrac{\partial u}{\partial \log_{10} z}\right)^2$

As already mentioned, four parameters φ_A, q_A, φ_B and q_B have inter-relations, so only one of them may be regarded as a representative. Therefore, we plotted φ_B against σ_A (Fig. 18), and we can see that σ_A is not so adequate.

A convenient graphical method for calculating the stability length L has been developed by Takeuchi.[13] With his results (Table 1), we

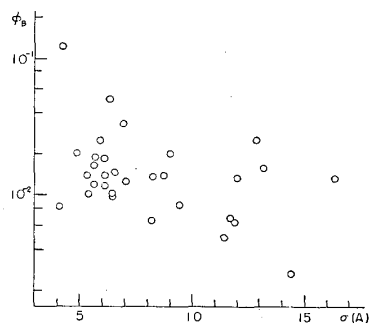

Fig. 18. Relation between φ_B and σ_A.

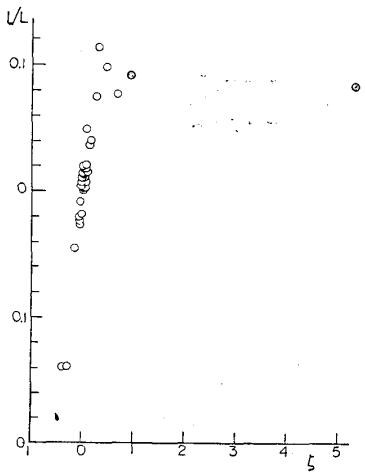

Fig. 19. Relation between 1/L and ζ.

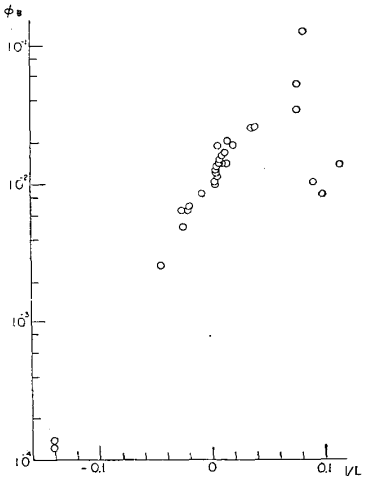

Fig. 20. Relation between φ_B and 1/L.

plotted ζ against 1/L and obtained Fig. 19; and we can see a close relationship between them. Furthermore, we plotted φ_B against 1/L and obtained Fig. 20. The points generally gather on a line, but they show some divergence at the larger part of 1/L in comparison with Fig. 15.

Results of other experiments

In the Tokai-experiments the relation between φ_A and ζ did not differ so remarkably (Fig. 13), but concerning with the vertical diffusion, φ_B (Fig. 15) or B_{1k} (value of B at 1 km.) (Fig. 21), differs considerably. Presumptive results calculated from Stewart's paper (Harwell)[6] were as follows:
Those calculated from Hay-Pasquill's paper (Porton)[4] were about 10 for every case. All these results are plotted in Fig. 21. This figure shows that even under unstable conditions ($\zeta<0$), results at Tokai, Harwell and Porton behave just like under the stable conditions ($\zeta<0$).

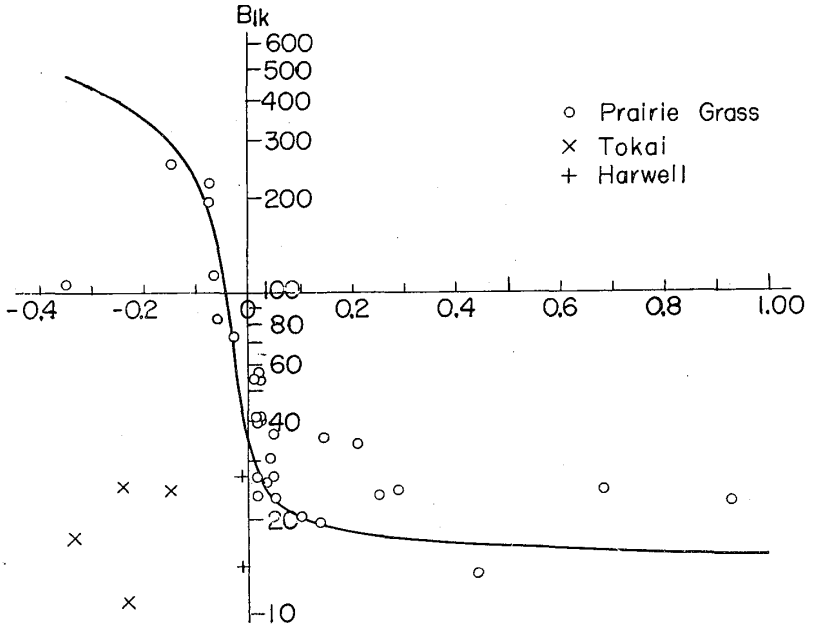

Fig. 21. Relation between B_1 and ζ.

Exp. No.	B_{1k}	ζ
F. 44	14	−0.02
F. 14	27	−0.01

Source height in Tokai-experiments was 65 m, that in Stewart's experiments was 61 m and those in Hay-Pasquill's experiments were ranging from 100 m to 150 m, while in Project Prairie Grass, it was

1.5 m.

The disturbances which are powerful for vertical diffusion may be caused by small air parcels which are rising owing to their buoyancies. The velocities of rising air parcels decrease as $z^{-0.29}$ [14]. Therefore, when the source height is higher, in order to be effective up to that height the disturbances must be powerful there, so the condition should be much more unstable. So it can be regarded that the above mentioned difference is due to the difference of source height. It may be a proof of this consideration that the values of B_{1k} have a relation with the source heights h. (Fig. 22)

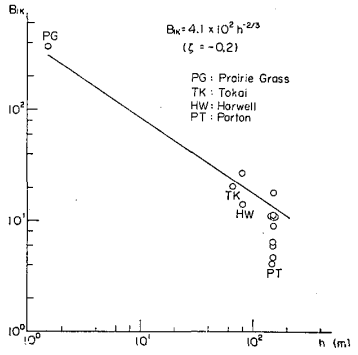

Fig. 22. Relation between B_{1k} and h.

The data ranging 40 km and 200 km of piled volcanic ashes of Mt. Asama have been reported by Minakami,[15,16] so we could analyse them and determine the horizontal diffusion parameters (Fig. 23).

Results for farther distances

The farthest observed distances in Tokai-experiments and in Project Prairie Grass are 3 km and 800 m respectively. There are scarcely any results ranging farther distances, so the extrapolation of the results to more farther distances may not be immediately admitted.

The data ranging 40 km and 200 km of piled volcanic ashes of Mt. Asama have been reported by Minakami,[15,16] so we could analyse them and determine the horizontal diffusion parameters (Fig. 23). If we plot these parameters from these results, togather with those from other experiments already mentioned, against the maximum observed

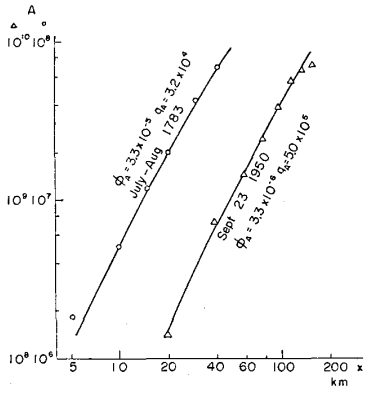

Fig. 23. Curves of A against x.

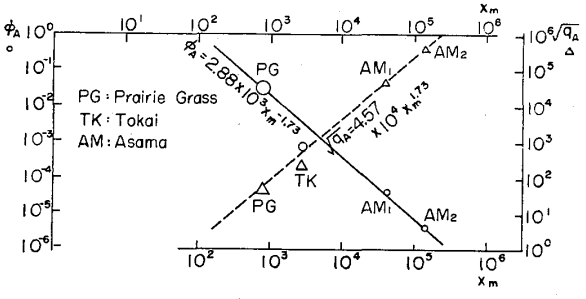

Fig. 24. Curves of φ_A and $\sqrt{q_A}$ against x_m.

distances, we get Fig. 24, which indicates that the magnitude of diffusion phenomena depends on the scale of the phenomena. For vertical diffusion, owing to the existence of the earth's surface, effective eddies do not become larger indefinitely; therefore, beyond a certain distance, e. g. 1 km, the diffusion parameters q and φ become independent on the scale of phenomena, and B should be regarded to be merely proportional to x.

Conclusion

Owing to the detailed data of the Project Prairie Grass, we could obtain fairly conclusive results. But there still remain many problems to be investigated, so we are longing for the chance of making further field experiments.

Acknowledgements

The author wish to express his deepest thanks to Dr. M. L. Barad for his consideration of sending to the author the reports of 'Prairie Grass Project' which gave him the motive to carry out this research. Furthermore, the author is sincerely grateful to the members of Research Group of Atmospheric Turbulence, especially Dr. E. Inoue, Dr. M. Shiotani, Mr. K. Imai, Mr. K. Takeuchi and Mr. K. Naito; and the members of the Investigation Committee of Atomic Energy and Meteorology, especially Dr. M. Ota, Mr. Y. Sasaki, Mr. S. Ito and Mr. N. Yokoyama for their earnest discussions.

References

1) Roberts, O. F. T.: Proc. Roy. Soc., A 104 1923 p. 640.
2) Sutton, O. G.: Proc. Roy. Soc., A 135 1932 p. 143.
3) Bosanquet, C. H.: and Pearson, J. L.: Trans. Faraday Soc., 32 1936 p. 1249.
4) Hay, J. S. and Pasquill, F.: J. Fluid Mech., 2 1957 p. 290.
5) Sakagami, J.: J. of Met. Soc. Japan, II 19 1941 p. 1 (in Japanese). Natural Sci. Rep., Ochanomizu Univ., 5 1954 p. 79.
6) Stewart, N. G. et al: AERE Harwell/JYH HD/32 1954.
7) Chamberlain, A. C.: AERE Hp/R 1261 1955.
8) Cramer, H. E. et al. Final Rep. No. AF 19(604)-1058, G. R. D. 1958.
9) Barad, M. L.: 'Atmospheric Diffusion and Air Pollution' Academia Press, 1959 p. 389.
10) Barad, M. L.: Geophy. Res. Papers, No. 59, G. R. D. 1959.
11) Sakagami, J.: Rep. No. 92 Inv. Comm. Atom. Ener. Met. 1959 (in Japanese). This will be published in J. Met. Soc. Japan in near future.
12) Taylor, G. I.: Proc. London Math. Soc., A 20 1921 p. 196.
13) Takeuchi, K.: J. Met. Soc. Japan II 38 (6) (to be published).
14) Sutton, O. G.: 'Micrometeorology' McGraw-Hill 1953 p. 300.
15) Minakami, T.: Bull. Earthquake Res. Inst., 20, 1943 p. 93.
16) Minakami, T. and Sakuma, S.: Bull. Volcanologique II 14 1953, p. 79.

(*Received Spet. 1, 1960*)

"On the Relations between the Diffusion Parameters and Meteorological Conditions"

ERRATA

Page	Line		Read
127	12	that value	what value
	24	may	many
128	22	$\frac{e^{-}}{\sqrt{A\pi}}$	$\frac{e^{-}}{\sqrt{A\pi}\sqrt{B\pi}}$
	32	$\frac{Q}{u}$	$\frac{Q}{u\sqrt{A\pi B}}$
129	7	distances	distance
	(foot noto) 2	coefficents	coefficients
137	11	are	arc
	13	$\int_{t_1+\xi}^{t_1+\xi+tx}$	$\int_{t_1+\xi-tx}^{t_1+\xi}$
	14	eqq	eqs
	22	$\overline{u}\left\|\int_{t_1+\xi}^{t_1+\xi+tx}\right\|=\overline{u}\left\|\int_{t_1}^{t_1+tx}\right\|$	$\overline{u}\left\|\int_{t_1+\xi-tx}^{t_1+\xi}\right\|=\overline{u}\left\|\int_{t_1-tx}^{t_1}\right\|$
138	4	L	L^2
	27	$\int_{t_1+\xi}^{t_1+\xi+x/\overline{u}}$	$\int_{t_1+\xi-x/\overline{u}}^{t_1+\xi}$
139	5	L	L^2
	8	will	may
140	1	q_A	$\sqrt{q_A}$
	(Run 21)	1.01^2	3.1^1
	(Run 37)	2.02	2.05
	(Run 43)	1.0^{-3}	2.0^{-3}
	(Run 46)	3.30^2	1.32^2
	(Run 67)	6.1^1	7.1^1
	(lowest)	9.2×10^{-3}	9.2×10^{-2}
149	2	$e^{\frac{\frac{h}{B}(\ )}{\sqrt{4\pi B h\sqrt{\ }}}}$	$\frac{e^{-\frac{h}{B}(\ )}}{\sqrt{4\pi B h\sqrt{\ }}}$
150	12	azumuthal	azimuthal
157	9	(Fig.21), differs	(Fig. 21) differs
	11~12	(insert the table on lines 15~17)	
158	13~17	(cross off)	
159	43	*spet*	*Sept*